U.PORTO

FACULDADE DE CIÊNCIAS
UNIVERSIDADE DO PORTO

Analytic Models for Realistic Cosmic Strings

Ana Almeida

Dissertação de Mestrado apresentada à
Faculdade de Ciências da Universidade do Porto em
Astronomia e Astrofísica

2021

Analytic Models for Realistic Cosmic Strings

Ana Almeida
Mestrado em Astronomia e Astrofísica
Departamento de Física e Astronomia
2021

Orientador
Carlos José Amaro Parente Martins,
Investigador Coordenador, Centro de Astrofísica da Universidade do Porto

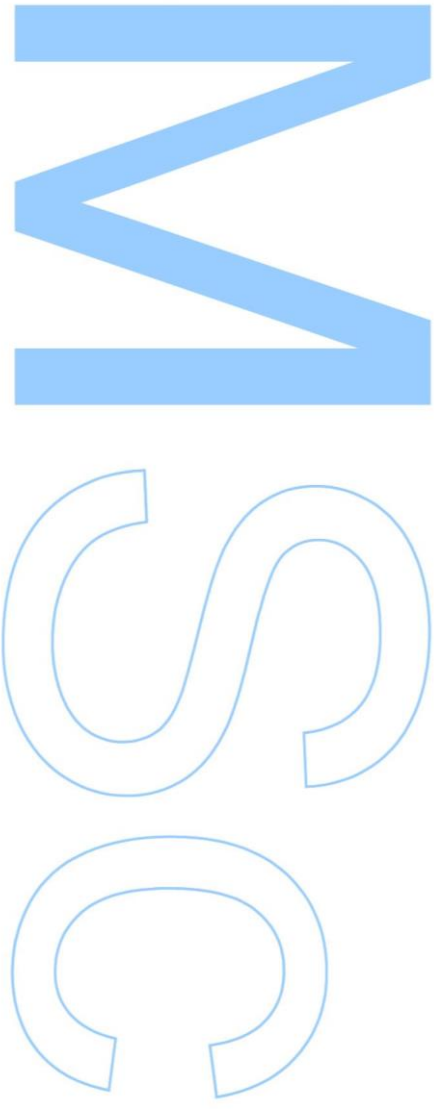

U.PORTO

FACULDADE DE CIÊNCIAS
UNIVERSIDADE DO PORTO

Todas as correções determinadas pelo júri, e só essas, foram efetuadas.

O Presidente do Júri,

Porto, _____/_____/_____

Acknowledgements

I would like to acknowledge all those who made the successful completion of this dissertation possible. I would first like to thank my supervisor, Dr. Carlos J. A. P. Martins, for all his guidance and precious physical insight, as well as for providing me with amazing scientific opportunities that allowed me to grow and learn more about this academic field. I would also like to acknowledge my colleagues from the Cosmoespresso project and in particular, José Ricardo Correia, for his continuous support.

Moreover, I would like to express my gratitude towards my colleagues and Professors from my Astrophysics Degree, from whom I learned so much throughout my academic studies. I would particularly like to thank Professor Catarina Lobo for her encouragement in the pursuit of an academic career.

Lastly, my appreciation goes out to my family and my friends. In particular, I want to thank my friends João Oliveira and Luís Trindade, for their endless support and patience, even in the darkest of times like the past year proved to be.

Dedicated to my grandparents.

Abstract

Cosmic string networks arise in many theories of unification beyond the standard model. In the context of cosmology, they are predicted to have been formed in the early universe as a consequence of the Kibble mechanism. The evolution of the simplest networks is quantitatively described by the canonical Velocity Dependent One-Scale (VOS) model. However, previous simulations of cosmic strings in expanding universes have demonstrated the existence of wiggles: significant amounts of short-wavelength propagation modes found on very small scales that have an impact on the network's evolution, as well as on its observational consequences. This motivated the development of a wiggly extension of the VOS. In this dissertation, we improve the physical interpretation of this model through a mathematical exploration of the landscape of possible scaling solutions. The modeling of the network's evolution relies on three main mechanisms: the universe's expansion rate, energy transfer mechanisms (e.g., the production of loops and wiggles), and the choice of the scale in which wiggles are coarse-grained. We consider the various limits where each mechanism dominates and compare the scaling solutions for each case, so as to gain insight into the roles of each mechanism in the overall behavior of the network. Besides the well-known Goto-Nambu solution, we find other non-trivial scaling regimes, where small-scale structure is able to build up in the network or reach scaling. We also determine the physical conditions that dictate each scaling regime, namely the allowed range of expansion rates and the relation between energy loss parameters. Our results demonstrate that full scaling of the network, including the wiggliness, is more likely in the matter era than in the radiation epoch, which is in agreement with numerical simulations. Lastly, our results are also compatible with the linear scaling observed in Minkowski space simulations.

Keywords: Cosmology, Topological Defects, Cosmic Strings

Resumo

As redes de cordas cósmicas surgem como consequência de várias teorias de unificação para além do Modelo Padrão de Física de Partículas. No contexto da cosmologia, a sua formação ocorre nos primórdios do universo, estando intimamente ligada ao mecanismo de Kibble. A evolução das redes de cordas mais simples é quantitativamente descrita pelo modelo canónico *Velocity Dependent One-Scale* (VOS). No entanto, tal como demonstrado por simulações de redes em universos em expansão, existem quantidades significativas de modos de propagação de baixo comprimento de onda encontradas em escalas muito pequenas, chamados *wiggles*. Esta estrutura de pequena escala tem impacto tanto na evolução da rede, como nas suas consequências observacionais. Tal levou ao desenvolvimento de uma extensão *wiggly* do modelo VOS. Com esta dissertação, pretende-se melhorar a interpretação física deste modelo através de uma exploração matemática das soluções de *scaling* do modelo. A evolução da rede de cordas depende essencialmente de três mecanismos: a expansão do universo, mecanismos de transferência de energia inerentes à rede, como a produção de loops e wiggles, e a escolha da escala em que as wiggles estão definidas. Assim, são considerados os vários limites em que cada mecanismo da rede é dominante, e são comparadas as soluções de *scaling* obtidas para cada caso, como forma de ganhar intuição acerca da função que cada mecanismo desempenha no comportamento da rede. Para além da solução conhecida de Goto-Nambu, são exploradas outras soluções de *scaling*: a estrutura de pequena escala cresce à medida que a rede evolui, ou evolui para um valor constante. São determinadas também as condições físicas que ditam cada regime de *scaling*, nomeadamente, a gama de taxas de expansão possíveis e a relação entre os parâmetros de perdas de energia. Os nossos resultados demonstram que um regime de *scaling* linear da rede é muito mais provável na era da matéria, do que na era da radiação, o que está de acordo com os resultados de simulações numéricas prévias. Por último, os nossos resultados são compatíveis com o scaling linear observado em simulações no espaço de Minkowski.

Palavras-chave: Cosmologia, Defeitos Topológicos, Cordas Cósmicas

Contents

List of Figures

List of Abbreviations

CMB	Cosmic Microwave Background
GR	General Relativity
FRW	Friedmann–Robertson–Walker
GUT	Grand Unified Theory
VOS	Velocity-Dependent One-Scale
RMS	Root-mean-square

Chapter 1

Introduction to Cosmic Strings

The purpose of this chapter is to provide the reader with an introduction to modern cosmology and an outline of the theoretical foundations behind topological defects, with an emphasis on cosmic strings. For a more comprehensive approach on the subject of defects, we refer the reader to [1]. In the cosmology introduction, we followed [2].

1.1 The Standard Model of Cosmology

The Standard Model of Cosmology is built upon the Cosmological Principle, which asserts that the universe exhibits homogeneity and isotropy on large scales. Having been formulated initially based on theoretical simplicity, this assumption is now supported by a robust bulk of evidence, the strongest being the uniformity of the Cosmic Microwave Background (henceforth CMB). On the basis of the symmetries embedded in the Cosmological Principle, Robertson and Walker were able to derive a general form of a spacetime metric, which had already been studied by Friedmann as an exact solution to the Einstein field equations of General Relativity (GR). The line element induced by the Friedmann–Robertson–Walker (FRW) metric, expressed in polar coordinates, yields:

$$ds^2 = a^2(t)\left[d\tau^2 - \frac{dr^2}{1-kr^2} - r^2 d\theta^2 - r^2 \sin^2\theta d\phi^2\right], \tag{1.1}$$

where τ is the conformal time which relates to the cosmic time t by $d\tau \equiv \frac{dt}{a(t)}$; k a constant associated to the curvature of space which can take values of $k = 0, +1, -1$, for a flat, closed and open space respectively; and $a(t)$ the scale factor. Here, we have adopted the (+,-,-,-) metric signature.

The scale factor encodes how the distance between points of a spatial hypersurface evolves in time. This motivates the following definition of the expansion rate of the universe (also known as the Hubble parameter H)

$$H \equiv \frac{\dot{a}}{a}, \tag{1.2}$$

where the dot denotes derivative with respect to cosmic time. Alternatively, one can also infer the expansion of the universe through the cosmological redshift z, defined as:

$$1 + z(t) \equiv \frac{a(t_o)}{a(t)}. \tag{1.3}$$

It is also convenient to introduce the notion of a cosmological horizon, which defines the maximum value of the radial coordinate r from which an observer at a given time t can receive light signals

$$d_H = a(t) \int_0^t \frac{dt'}{a\,(t')} \tag{1.4}$$

In a FRW model, this integral converges, yielding a horizon size of $d_{\rm H} = 3t$ in the matter dominated era, and $d_{\rm H} = 2t$ in the radiation era (both assuming flat geometry).

The expansion of the universe is assumed to be dictated by Einstein equations

$$R_{\mu\nu} - \frac{1}{2} R g_{\mu\nu} = 8\pi G T_{\mu\nu}, \tag{1.5}$$

where G is Newton's gravitational constant, $R_{\mu\nu}$ is the Ricci tensor, R the Ricci scalar and $T_{\mu\nu}$ the stress energy-momentum tensor. For the FRW metric, the Einstein field equations yield:

$$H^2 = \frac{8\pi G}{3}\rho - \frac{k}{a^2}, \tag{1.6}$$

which is formally known as the Friedmann equation, and:

$$\frac{\ddot{a}}{a} = -\frac{4\pi G}{3}(\rho + 3p), \tag{1.7}$$

which simply expresses the conservation of the energy–momentum tensor:

$$\dot{\rho} + 3H(\rho + p) = 0, \tag{1.8}$$

where p and ρ are the fluid's pressure and energy density, respectively. A key assumption that underlies the standard cosmological paradigm is that the distribution of matter of the universe can be modeled as a homogeneous and isotropic perfect fluid (inviscid, no heat conduction). Perfect fluids are completely characterized by their pressure and energy

density, which are related by the equation of state parameter w

$$p = w\rho. \tag{1.9}$$

Employing this equation of state in Eq. (1.8), assuming a constant w, we find

$$\rho \propto a^{-3(w+1)}. \tag{1.10}$$

Further assuming flat geometry $k = 0$, it can also be shown that solutions of (1.6) take the simple form:

$$a \propto t^{\frac{2}{3(w+1)}}. \tag{1.11}$$

Non-relativistic matter can be approximated to a pressureless fluid ($w = 0$), and so, in the matter-dominated era the scale factor evolves according to $a \propto t^{2/3}$, while for a relativistic fluid, like the one that dominated the radiation era of the universe, one has $w = \frac{1}{3}$, yielding $a \propto t^{1/2}$.

A crucial development in the model came with Edwin Hubble's 1929 discovery that our universe is expanding. The astronomer Vesto Slipher had already discovered in 1910 that the spectral lines of most spiral nebulae exhibited redshift, thus implying that these objects were receding, but it was Hubble that established a linear relation between the galaxy's distance and their recessional velocities (the proportionality factor being H_o). In other words, the farther a galaxy was, the faster it was moving away, which is indicative of a cosmological expansion. The Standard Model of Cosmology is also sustained by two additional observational pillars. Perhaps one of the most important discoveries that propelled observational cosmology into its "Golden Age" was the 1965 discovery of the CMB by Arno Penzias and Robert Wilson. The CMB is electromagnetic radiation that originated upon the decoupling of photons from matter that took place in the so-called epoch of recombination of the early universe. Another important observational discovery was the measure of the abundances of hydrogen and helium, which were in excellent agreement with the theoretical calculations made by George Gamow and Ralph Alpher.

But modern cosmology reaches far beyond the already discussed foundations, being one of the branches of physics with the most growth in the last decades. An important breakthrough that revolutionized the field came with the realization that the visible matter of the universe was only a small piece of the puzzle. As yielded by the best fit to CMB anisotropy spectrum data, the universe has 27% of its mass-energy content in the form

of cold dark matter, a new type of matter that does not seem to interact with the electromagnetic field, with baryonic matter accounting for only the small fraction of 5% [3]. More surprisingly, the remaining 68% lies in an unexplainable energy component: dark energy (or cosmological constant Λ), which is believed to be responsible for the recent acceleration of the universe. This is the simplest theoretical framework that is coherent with observations and it is known as the ΛCDM model. Despite the remarkable concordance, there are still a number of unsolved questions in this model. One critical open question is whether topological defects are formed during the phase transitions that the primordial universe underwent, as theorized in particle physics theories, and in spite of no observational confirmation.

1.2 Topological Defects in Cosmology

Topological defects feature in many high energy physics models, but it is perhaps in their cosmological application that they are the most interesting, as stable defects can provide unique insights into the early universe conditions. To put it simply, defects consist of discontinuities in the scalar field due to spontaneous symmetry breaking during the phase transitions of the early epochs of the universe [1, 4]. The word "defects" is owed to those discontinuities, while "topological" stems from the use of the mathematical field of topology in order to describe some symmetry concepts.

1.2.1 Spontaneous Symmetry Breaking

The concept of symmetry, that is, the notion that the laws that govern a system remain invariant under a given symmetry transformation, lies at the heart of many theories in physics. A symmetry is mathematically described by an abstract object called a group G, which is essentially a set within which a product operation is defined, such that it fulfills three requirements (associativity, identity, and the existence of an inverse element within the group). Symmetries that vary in spacetime are known as local, while symmetries that are constant are global.

The mechanism of spontaneous symmetry breaking is explained in terms of the Higgs scalar field ϕ. Suppose the Lagrangian of a theory is invariant under the action of G. A symmetry is said to be spontaneously broken when ϕ adopts an expectation value $\langle\phi\rangle$

which is only invariant under a smaller number of symmetries, leading the larger symmetry group G to break into a smaller one, the unbroken group H

$$G \longrightarrow H, \tag{1.12}$$

where H is given by:

$$H = \{g \in G : D(g)\phi = \phi\}, \tag{1.13}$$

where $D(g)$ is a representation of G, a homomorphism from G to the group of $n \times n$ complex invertible matrices $GL(n, \mathbb{C})$

$$D : G \longrightarrow GL(n, \mathbb{C}),$$

$$\forall g_1, g_2 \in G, \quad D(g_1) \cdot D(g_2) = D(g_1 \cdot g_2). \tag{1.14}$$

Group representations are useful, as they map group elements onto variables with physical meaning.

This mechanism is understood as a phase transition because the temperature-dependent potential $V(\phi, T)$ develops non-trivial minima, responsible for breaking the symmetry. At sufficiently large temperatures $T > T_c$ (T_c being the critical temperature), the symmetry is restored, as the Higgs scalar field is in a symmetric state (known as the old or false vacuum), with vanishing expectation value everywhere $\langle\phi\rangle = 0$. But for temperatures below the critical temperature $T < T_c$, the old vacuum is no longer stable, leading $V(\phi)$ to favor non-trivial minima at which $\langle\phi\rangle \neq 0$ (the new or true vacuum), and thus spontaneously breaking the symmetry. This set of degenerate minima form the vacuum manifold $\mathcal{M}$, which is recognized as the coset space

$$\mathcal{M} = G/H. \tag{1.15}$$

These concepts can be illustrated by considering the simple Goldstone model [5] for a complex scalar field ϕ, whose Lagrangian density is

$$\mathcal{L} = \left(\partial_\mu \bar{\phi}\right)\left(\partial^\mu \phi\right) - V(\phi), \tag{1.16}$$

with $V(\phi)$ being the following potential

$$V(\phi) = \frac{1}{4}\lambda(\bar{\phi}\phi - \eta^2)^2, \tag{1.17}$$

where λ and η are positive constants. In this case, the symmetry group G corresponds to

the group of one-dimensional unitary complex matrices formally denoted $U(1)$, implying Eq. (1.16) is invariant under symmetry transformations of the type $\phi(x) \rightarrow e^{i\alpha}\phi(x)$ (α being a constant that does not depend on spacetime coordinates). This potential is minimized by two symmetric states $\phi = \pm\eta$, which form the vacuum manifold $\mathcal{M}$.

1.2.2 The Kibble mechanism

The production of defects during cosmological phase transitions is explained by the Kibble mechanism [4]. As the universe expands and cools off, it eventually reaches T_c, at which ϕ rolls down the potential towards the degenerate ground states. Fluctuations of either thermal or quantum origin play a role in this choice of minima. However, not all fluctuations will be correlated, as causality implies that regions of space separated by distances greater than the cosmological horizon will be uncorrelated. As a consequence, outside the correlation area defined by $\xi < t$, ϕ will have arbitrary values. When regions with different values of ϕ merge, topological defects form.

1.2.3 Classification of Topological Defects

The nature of the topological defect is determined by the topology of the vacuum manifold $\mathcal{M}$ [4]. More precisely, defect classification relies on homotopy theory, whose main idea is that $n-$dimensional loops defined on manifolds can be arranged into equivalence classes based on how they deform. Loops that can be continuously deformed into each other are part of an equivalence class. In this case, the deformation is said to be a homotopy, and the loops within the equivalent class are homotopically equivalent. Conversely, loops of different classes can not be deformed into each other. Equivalence classes can be demonstrated to form a group formally known as the n^{th}-homotopy group $\pi_n(\mathcal{M})(n = 0,1,2,3)$. The elements of $\pi_n(\mathcal{M})$ have a correspondence to the type of defect formed (although not always one-to-one).

Considering the previous Goldstone model, the spontaneous breaking of a discrete symmetry originates a vacuum manifold that is disconnected, that is, its zeroth homotopy group is not trivial $\pi_0(\mathcal{M}) \neq I$ (I being the trivial group). This type of defect is known as a domain wall, a two-dimensional surface that separates regions with different orientations of the Higgs field. Defects can also take the form of cosmic strings, which arise when the first homotopy group, also known as the fundamental group, is non-trivial

$\pi_1(\mathcal{M}) \neq I$, implying the vacuum manifold is not simply connected, that is, it has unshrinkable loops. Monopoles are point-like defects for which $\pi_2(\mathcal{M}) \neq I$, implying there are non-contractible surfaces in the vacuum manifold. Both domain walls and monopoles are excluded from being realistic, at least if formed at high energies, because models in which their formation is predicted imply that they would overclose the universe, causing it to collapse early and thus, preventing it from reaching its current age. Lastly, one can also have textures which originate when $\pi_3(\mathcal{M}) \neq I$, or equivalently, $\mathcal{M}$ contains non-contractible three-spheres. One aspect that sets textures apart from the other defects is the fact that the field is in the vacuum manifold at every point in space, as opposed to what occurs with strings, monopoles, and domain walls, where the vacuum manifold is confined within a well-defined core.

Moreover, defects can also be classified as global or local depending on their original symmetry group. For defects produced by gauge symmetries, the presence of gauge fields annihilates the gradients of the scalar field $\partial_\mu \phi$, yielding a null covariant derivative $D_\mu \phi = 0$ outside the vacuum manifold and thus confining the old vacuum to a well-defined region. This is not the case for global defects, where one has to account for the long-range forces originated by massless bosons.

1.3 Cosmic Strings

1.3.1 Basic Properties and Dynamics

Cosmic strings emerge when the field traces a closed curve around the vacuum manifold that is non-contractible in $\mathcal{M}$. In other words, there exists a point at which the loop can not be further contracted without that implying departure from the vacuum manifold, and where field continuity imposes $\phi = 0$. As the system tries to minimize the gradient energy of the scalar field, these points take up a line-like configuration, thus forming a cosmic string.

The width of a string is given by

$$\delta \sim (\sqrt{\lambda}\eta)^{-1} \sim m_\phi^{-1}, \tag{1.18}$$

where m_ϕ is the Higgs mass. The string's mass per unit length μ_o can be identified with the symmetry breaking energy scale η

$$\mu_o \sim \eta^2, \tag{1.19}$$

having no dependence on the coupling constant λ. Strings are completely characterized by μ_o, which is equal to the string tension T for simple strings with no additional degrees of freedom. Having been formed very early in the history of the universe, they are capable of storing large quantities of mass-energy, in spite of usually being very thin objects. For strings born in the GUT Epoch of the Universe, μ_o is around the order of $\mu_o \sim 10^{21} kgm^{-1}$, with a corresponding thickness of $10^{-24} m$ [6].

Strings can not possess extremities given that would create discontinuities in the field. Consequently, they can either take the form of infinite strings or loops. As a consequence of the Kibble mechanism, strings are expected to form networks that survive throughout time and that could theoretically overdominate the universe. But, evidently, this does not correspond to what is observed. This is because a realistic scenario of a cosmological string network can only be possible by taking into consideration the various ways by which the network loses energy. As it will become apparent later, the energy loss phenomena inherent to the network plays an important role in the network's evolution. Strings can lose their energy by radiation decay and by intersecting with other strings or even themselves, and they can also intercommute, which is when the extremities of a string segment disconnect and attach to another segment at the point of intersection. These interactions can result in the formation of closed loops and singularities like kinks and cusps.

1.3.2 Astrophysical Consequences

Defects may pervade in condensed matter physics, but they remain entirely hypothetical in cosmology as their observational confirmation is yet to occur. Nevertheless, they still constitute objects of immense interest to cosmology. From a theoretical point of view, primordial strings could be the main source responsible for baryogenesis [7]; and string loops may have played a part in the formation of supermassive black holes [8]. Furthermore, the astrophysical imprint left by strings can also contribute to our knowledge of particle physics by creating opportunities to probe energy scales beyond what is currently allowed with particle accelerators, as the greater the value of μ_o, the higher the energy scale one is dealing with.

Many of the constraints derived on the string tension are based on the string's gravitational signatures. The presence of a string influences the surrounding spacetime geometry, inducing a deficit angle $\alpha = 8\pi G\mu_o$, such that a complete rotation around the string

yields an angle of $2\pi - \alpha$. One of the ways in which this manifests, serving as an indirect detection method, is that strings behave as cylindrical gravitational lenses with a singular and identifiable signature compared to other astrophysical lensing events. Straight long strings are predicted to produce two identical images of the light sources, with no distortion and with an expected angular separation of $\delta\theta \sim \alpha$ [9]. Because detection through the string's lensing action is independent of model choice, it is one of the best methods. Nevertheless, the detection still proves to be an arduous task, with there having been various candidates [10] [11] that were all later excluded and attributed to other astrophysical phenomena.

Another signature comes from the CMB anisotropies caused by string defects. Because a string in motion will cause a relative velocity between a source of photons and an observer, photons will suffer a Doppler shift of $\frac{\delta T}{T} \sim 8\pi G\mu_o v_\perp$ (where $v_\perp$ is the component of the string's velocity that is perpendicular to the plane formed by the string and the observer's line of sight). Due to the deficit angle, the redshift will be different depending on the photon's direction, which would leave line-shaped discontinuities in the CMB temperature, an effect known as the Kaiser-Stebbins Effect [12, 13]. Another gravitational effect is the formation of an overdense wedge-like region, known as a wake, behind a string that is in motion [14]. Even though this provides an interesting mechanism for structure formation, we know strings can only have a minor contribution in this process, as the observed power spectrum of anisotropies of the CMB differs substantially from the one expected from strings.

Furthermore, strings are capable of emitting gravitational radiation [15]. Specifically, long strings and loops are expected to generate a stochastic background of gravitational waves in the primordial universe, which gravitational wave observatories could probe [16]. Kinks and cusps are also expected to dissipate energy through gravitational wave emission. But the strongest constraint to date is yielded by observations of the timing of millisecond pulsars $G\mu_o \lesssim 10^{-10}$ [17, 18]. The reasoning behind this constraint is based on the perturbations in the timing of pulsars owed to the gravitational wave background originated by loops.

On a final important note, it should be said that these scenarios are oversimplified, as they do not take into account the complexity that is inherent to realistic networks of strings, such as the small-scale structure that inevitably emerges, or the mere fact that strings are dynamic and have curvature. As seen in the next chapters, the presence of

small-scale structure interferes with the network's evolution, thus affecting its observational imprint.

Chapter 2

Evolution of Goto-Nambu and Wiggly Cosmic Strings

In this chapter, we begin with a brief examination of the Velocity-Dependent One-Scale (VOS) description of Goto-Nambu strings, followed by a motivation of the necessity for model extensions that account for the string's non-trivial internal structure. Finally, we discuss the wiggly extension of the VOS, following the formalism developed by [19, 20].

Having established the importance that cosmic strings have in our understanding of the early phases of the universe, we are now concerned with their evolution. Because of their complexity and non-linearity, it is only through an in-depth study of the evolution of their networks that their cosmological implications can be truly understood. This study is carried out by two complementary approaches: numerical simulations and analytic models. The usual methodology behind these models consists of using the statistical mechanics of the network in order to derive equations that account for the evolution of the large-scale quantities of the network, rather than having to deal with the complexity of the microphysics [6].The loss of information that comes with this procedure is encapsulated in the form of phenomenological parameters. The interplay between the computational and theoretical approaches is essential in order to have an accurate framework, as the model parameters are calibrated with the aid of numerical simulations.

2.1 Goto-Nambu Strings Evolution

2.1.1 The Velocity-Dependent One Scale (VOS) Model

The canonical framework for Goto-Nambu strings is the so-called VOS model [21, 22]. It provides a description of the evolution of the network in terms of two macroscopic quantities: a mean velocity v and a typical length scale L, that can be identified with the inter-string distance, the correlation length ξ, or the average curvature radius R. The VOS follows the same spirit embodied in the model originally developed by Kibble [23], which entails an equation that governs the dynamics of a single length scale under the assumption of $L = \xi = R$. Other models ensued, like the three-scale framework [24], but it was only with the advent of the VOS that a model capable of making robust predictions in various cosmological epochs emerged. Moreover, the VOS has been extensively tested against numerical simulations, further demonstrating its success and reliability [25–28].

We now show, in a very concise manner, how the dynamics equations for a network of long strings can be obtained. A thorough derivation can be found in [21, 22]. The starting point of this procedure is the variation of the effective Goto-Nambu action

$$S = -\mu_o \int \sqrt{-\gamma} d^2\sigma, \tag{2.1}$$

where σ represents the two-dimensional coordinates used to parametrize the string's worldsheet, and γ stands for the determinant of the worldsheet's metric, immersed in the background spacetime of metric $g_{\mu\nu}$ ($\mu, \nu = 0, 1, 2, 3$)

$$\gamma_{ij} = g_{\mu\nu} x^{\mu}_{,i} x^{\nu}_{,j}. \tag{2.2}$$

This is only correct provided one makes the assumption of the width being much smaller than the curvature radius. We also adopt a specific choice of gauge

$$\sigma^0 = \tau, \quad \dot{x}x' = 0, \tag{2.3}$$

with the prime designating derivative with respect to spatial worldsheet coordinates $x' \equiv \frac{dx}{d\sigma^1}$. It is convenient to introduce the coordinate energy per unit of length

$$\epsilon^2 = \frac{\mathbf{x}'^2}{1 - \dot{\mathbf{x}}^2}. \tag{2.4}$$

One can then demonstrate that the equations of motion in a FRW universe yield:

$$\ddot{\mathrm{x}} + 2\frac{\dot{a}}{a}\dot{\mathbf{x}}\left(1-\dot{\mathrm{x}}^2\right) = \frac{1}{\epsilon}\left(\frac{\mathrm{x}'}{\epsilon}\right)' \tag{2.5}$$

$$\dot{\epsilon} + 2\epsilon\frac{\dot{a}}{a}\dot{\mathbf{x}}^2 = 0. \tag{2.6}$$

In the VOS formalism, the dynamics of the network is described by the root-mean-square (RMS) velocity

$$v^2 \equiv < \dot{x}^2 > = \frac{\int \dot{\mathbf{x}}^2 \epsilon d\sigma}{\int \epsilon d\sigma}, \tag{2.7}$$

and the total energy of the network

$$E = a\mu_o \int \epsilon d\sigma. \tag{2.8}$$

For Brownian long strings, one can define a characteristic length L and so one can express the energy in terms of L, making use of the following relation:

$$\rho_\infty = \frac{E}{a^3} \equiv \frac{\mu}{L^2}. \tag{2.9}$$

As far as the phenomenological parameters are concerned, the fraction of energy lost into the production of loops is encoded in a loop chopping efficiency parameter c.

$$\left(\frac{1}{\rho}\frac{d\rho}{dt}\right)_{loops} = \frac{cv}{L}. \tag{2.10}$$

Because strings are not perfectly straight, an additional parameter that quantifies their local curvature is needed, motivating the definition of the momentum parameter

$$k(v) \equiv \frac{\langle (1-\dot{\mathbf{x}}^2)(\dot{\mathbf{x}}\cdot\mathbf{u})\rangle}{v(1-v^2)}, \tag{2.11}$$

with $\mathbf{u}$ being a unit vector whose direction is parallel to the curvature radius vector. Numerical simulations [29] suggest a simplified version of Eq. (2.11), valid for relativistic strings:

$$k_{\mathrm{r}}(v) = \frac{2\sqrt{2}}{\pi}\frac{1-8v^6}{1+8v^6}, \tag{2.12}$$

which takes the value of unity for a straight string. The low number of parameters ensures the model is still predictive.

Having introduced all the required phenomenological parameters, we are now set to derive the equations of motion. Through differentiation of Eq. (2.8) and making use of Eq. (2.10), we obtain the differential equation that describes how the network's characteristic

length scale evolves in time:

$$\frac{dL}{dt} = HL(1+v^2) + \frac{1}{2}cv, \tag{2.13}$$

The physical interpretation of this equation is clear: the string is stretched with Hubble expansion and loop formation. Analogously, one finds the equation for the evolution of the RMS velocity by differentiation of Eq. (2.7)

$$\frac{dv}{dt} = (1-v^2)\left[\frac{k(v)}{L} - 2Hv\right], \tag{2.14}$$

which is simply Newton's Second Law stating the string is accelerated by its curvature but decelerated by Hubble expansion that acts as a damping term. Having developed the two differential equations (2.13)(2.14) that compose the VOS, we now turn our analysis to the relevant scaling solutions.

2.1.2 Scaling Solutions

The realistic scenarios one expects for networks of strings are described by scaling solutions where the small-scale dynamics (e.g. production of loops) balance the large-scale dynamics of the Hubble expansion, thus ensuring the network is not a dominant component of the universe's energy density. When the rate of energy loss is at the maximum that is allowed by causality, the network is said to have reached a scale-invariant solution [29], implying constant velocity and a characteristic length scale proportional to the cosmological horizon $L \propto H^{-1}$

$$L = \left(\frac{k(k+c)}{4\lambda(1-\lambda)}\right)^{1/2} t, \quad v = \left(\frac{k(1-\lambda)}{\lambda(k+c)}\right)^{1/2}, \tag{2.15}$$

resulting in the network's total energy being a constant fraction of the cosmological background:

$$\frac{\rho}{\rho_{crit}} \propto \text{const.} \tag{2.16}$$

(2.15) is a mathematical attractor, implying that the network always converges towards this equilibrium solution regardless of the initial conditions. However, this solution is only admissible when the expansion follows a power law $a \propto t^{\lambda}$, where the network is able to adjust to the evolution of the cosmological background.

2.2 Wiggly Strings Evolution

In spite of the triumphs of the VOS, the model is not sophisticated enough to depict the dynamics of networks of realistic strings, whose worldsheets have extra degrees of freedom (e.g., a charge current). This is because the underlying one-scale hypothesis of the VOS allows for only two evolution equations, leaving no room for descriptions of additional degrees of freedom on the worldsheet. However, it became increasingly evident from numerical simulations that the strings possessed non-negligible amounts of short-wavelength propagation modes (known as wiggles) at scales orders of magnitude below the correlation length. Even though this is partially induced by the simulations themselves, the presence of small-scale structure is a byproduct of the energy loss phenomena of the network, thus prompting the need for an extension of the VOS that describes these dynamics.

A wiggly extension of the VOS is accomplished by noting that, in direct contrast with Goto-Nambu strings, wiggly strings have their local string tension T differ from the energy density in the string's local rest frame U. In particular, this variation can be defined with the introduction of a parameter w that ranges from 0 to 1 (unity being the value of a Goto-Nambu string), such that

$$\frac{T}{\mu} = w, \quad \frac{U}{\mu} = \frac{1}{w}. \tag{2.17}$$

This motivates the redefinition of the total energy

$$E = a \int \epsilon U d\sigma = \mu_o a \int \frac{\epsilon}{w} d\sigma, \tag{2.18}$$

which can be decomposed into two contributions: one that lies in the bare string segments that will be denoted E_o,

$$E_o = \mu_o a \int \epsilon d\sigma, \tag{2.19}$$

and another owed to the wiggles E_w:

$$E_w = \mu_o a \int \frac{1-w}{w} \epsilon d\sigma. \tag{2.20}$$

The additional degree of freedom in the wiggly extension comes in the form of a renormalized string mass per unit length μ, which will yield a differential equation that accounts for small-scale structure evolution. μ is a measure of the energy due to the wiggliness of the network, so it is natural to define it as a ratio between the total energy of the

network and the energy in the bare string segments

$$\mu \equiv \frac{E}{E_o} \geq 1 \tag{2.21}$$

If we further define associating characteristic length scales to each energy contribution

$$\rho \equiv \frac{\mu_o}{L^2} \tag{2.22}$$

$$\rho_o \equiv \frac{\mu_o}{\xi^2}, \tag{2.23}$$

we can express μ as a ratio between length scales:

$$\mu = \left(\frac{\xi}{L}\right)^2. \tag{2.24}$$

This procedure makes it evident that a quantitative description of small-scale structure implies the departure from the one-scale assumption that holds in the VOS framework. Nevertheless, the wiggly model still assumes the correlation length is identified with the string curvature radius $\xi \sim R$, which can be verified via numerical studies [26]. It should also be emphasized that while ξ measures a physical length, L is only a convenient definition of a length that a Goto-Nambu string with equal total energy would have.

As with the VOS model, one needs to average the dynamical quantities over the network. In the formalism developed by [19, 20], the adopted procedure averaged the quantities over the total energy, so that string segments that carry greater mass currents have more weight. For a generic quantity Q, this is defined as:

$$\langle Q \rangle = \frac{\int QU\epsilon d\sigma}{\int U\epsilon d\sigma} = \frac{\int Q\frac{\epsilon}{w} d\sigma}{\int \frac{\epsilon}{w} d\sigma} \tag{2.25}$$

This is the method we follow, however it should be noted that an equally reasonable approach consists of averaging over the bare energy:

$$\langle Q \rangle_0 = \frac{\int Q\epsilon d\sigma}{\int \epsilon d\sigma}. \tag{2.26}$$

The two approaches are related by:

$$\langle Q \rangle = \frac{\langle QU \rangle_0}{\langle U \rangle_0} = \frac{\langle Q/w \rangle_0}{\mu}. \tag{2.27}$$

We still need to take into account the intrinsic energy transfers of the network, as some of them contribute to the generation of small-scale structure, while others are instrumental in its loss. The intercommutation of strings is followed by the appearance of discontinuities in the string's tangential direction, known as kinks, that increase the energy due to wiggles. This energy transfer from the bare string to the wiggles is quantitatively described by:

$$\left(\frac{1}{\rho_o}\frac{d\rho_o}{dt}\right)_{\text{wiggles}} = -cs(\mu)\frac{v}{\xi},, \tag{2.28}$$

in which s approaches 0 in the Goto-Nambu limit. Besides accounting for the gain in small-scale structure, s should also account for kink decay by gravitational radiation emission. Although the formation of kinks in the network is an independent process of loop production, intercommutation also originates loops. In fact, numerical simulations [26, 30, 31] hint at small-scale structure stimulating the production of loops, and therefore favoring the production of loops wherever kinks are formed on the network. With the appearance of these small-scale loops, the energy transfer from the network to loops contributes to the overall loss of small-scale structure on the network. Analogously to what was done in the Goto-Nambu case, these effects are quantified by a loop-chopping efficiency parameter. However, when doing so, one must distinguish two contributions: not only are loops produced directly from the string, but also from the wiggles. The fraction of bare energy density fraction lost into loops per unit time is then modeled as

$$\left(\frac{1}{\rho_o}\frac{d\rho_o}{dt}\right)_{\text{loops}} = -cf_o(\mu)\frac{v}{\xi}. \tag{2.29}$$

Note that in the Goto-Nambu limit $\mu \longrightarrow 1$, f_o approaches unity in order to retrieve (2.10). Conversely, the fraction of energy density owed to the wiggles is given by:

$$\left(\frac{1}{\rho_w}\frac{d\rho_w}{dt}\right)_{\text{loops}} = -cf_1(\mu)\frac{v}{\xi}, \tag{2.30}$$

such that total energy lost into loops comes

$$\left(\frac{1}{\rho}\frac{d\rho}{dt}\right)_{\text{loops}} = \left(\frac{1}{\rho}\frac{d\rho_0}{dt}\right)_{\text{loops}} + \left(\frac{1}{\rho}\frac{d\rho_w}{dt}\right)_{\text{loops}}. \tag{2.31}$$

For simplicity's sake, one can define an overall energy loss parameter

$$\left(\frac{1}{\rho}\frac{d\rho}{dt}\right)_{\text{loops}} \equiv -cf(\mu)\frac{v}{\xi}, \tag{2.32}$$

which using (2.29),(2.30),(2.31) can be shown to yield:

$$f(\mu) = \frac{f_o(\mu)}{\mu} + \left(1 - \frac{1}{\mu}\right) f_1(\mu). \tag{2.33}$$

In accordance with [20], we assume the previously discussed parameters take the form

$$\begin{aligned} f_o(\mu) &= 1 \\ f(\mu) &= 1 + \eta\left(1 - \frac{1}{\sqrt{\mu}}\right) \\ s(\mu) &= D\left(1 - \frac{1}{\mu^2}\right) \end{aligned} \tag{2.34}$$

where η and D are new phenomenological parameters that can be understood as probabilities for small-scale structure loss and gain, respectively.

We are finally ready to derive the evolution equation for small-scale structure. It should be noted that the renormalized string mass μ has an explicit dependence on time, but also on the renormalization scale $\mu = \mu(\ell, t)$ [26], which needs not be fixed and is expected to vary in time (e.g., the correlation length). In fact, the choice of scale is equivalent to altering what defines a wiggle, and consequently, must have a direct influence on the energy distribution between the bare string and the wiggles. This is done by introducing the scale-drift term in the differential equation for μ

$$\frac{1}{\mu}\frac{\partial \mu}{\partial \ell}\frac{d\ell}{dt} \sim \frac{d_m - 1}{l}\frac{d\ell}{dt}, \tag{2.35}$$

where the multifractal dimension of a string segment at scale ℓ is denoted by $d_m(\ell)$ [32]. A consequence of this procedure that one may not anticipate is that the velocity equation also needs to be modified, so as to ensure energy conservation at all scales, by including the following term

$$\frac{\partial v^2}{\partial \ell}\frac{d\ell}{dt} = \frac{1 - v^2}{1 + \langle w^2 \rangle}\frac{\partial \langle w^2 \rangle}{\partial \ell}\frac{d\ell}{dt}, \tag{2.36}$$

Here we witness another departure from the VOS, as this implies that v is to be interpreted as a mesoscopic quantity, which contrasts with the traditional VOS interpretation of a microscopic velocity. In particular, in what follows we adopt the following phenomenological relation

$$d_m(\mu) = 2 - \frac{1}{\mu^b}, \tag{2.37}$$

with b being a free parameter that imposes the transition limit between two regimes ($d_m = 2$ for Brownian networks, $d_m = 1$ for small scales). Numerical simulations [26] suggest

the value of $b = 2$ is reasonable.

The following system of equations that compose the wiggly extension of the VOS is then derived:

$$2\frac{dL}{dt} = HL\left[3 + v^2 - \frac{(1-v^2)}{\mu^2}\right] + \frac{cfv}{\sqrt{\mu}} \tag{2.38}$$

$$2\frac{d\xi}{dt} = H\xi\left[2 + \left(1 + \frac{1}{\mu^2}\right)v^2\right] + v\left[k\left(1 - \frac{1}{\mu^2}\right) + c\left(f_o + s\right)\right] + \left[d_m\left(\ell\right) - 1\right]\frac{\xi}{\ell}\frac{d\ell}{dt} \tag{2.39}$$

$$\frac{dv}{dt} = \left(1 - v^2\right)\left[\frac{k}{\xi\mu^2} - Hv\left(1 + \frac{1}{\mu^2}\right) - \frac{1}{1+\mu^2}\frac{\left[d_m\left(\ell\right) - 1\right]}{v\ell}\frac{d\ell}{dt}\right] \tag{2.40}$$

$$\frac{1}{\mu}\frac{d\mu}{dt} = \frac{v}{\xi}\left[k\left(1 - \frac{1}{\mu^2}\right) - c\left(f - f_o - s\right)\right] - H\left(1 - \frac{1}{\mu^2}\right) + \frac{\left[d_m\left(\ell\right) - 1\right]}{\ell}\frac{d\ell}{dt}. \tag{2.41}$$

It should be noted that due to the relation between μ, L and ξ described by Eq. (2.24), only three of these equations are independent.

Chapter 3

Scaling Solutions of Wiggly Cosmic Strings

In this chapter, we seek to deepen our understanding of the dynamics of wiggly cosmic strings. We accomplish this by studying the allowed solutions of the wiggly generalization of the VOS, and attempting to comprehend their physical implications.

Specifically, we carry out a systematic study of the asymptotic scaling solutions of the wiggly extension of the VOS, as a way to gain a deeper understanding of the physics that governs wiggly strings. One key question that remains unanswered is whether small-scale structure reaches scaling and under what physical conditions. Numerical simulations [26] suggest that scaling is attained at least in the matter-dominated era. The interpretation in the radiation era is less evident, which may be indicative of the nonexistence of a scaling solution, or a slower scaling regime in the presence of less Hubble damping. Nevertheless, this motivates the exploration of the non-trivial solutions (other than the well-known Goto-Nambu solution).

As depicted by the dynamics equations (2.38)-(2.41), the evolution of the network is driven by three main mechanisms: the universe's expansion, energy loss by intercommutation, and the choice of the scale in which wiggles are coarse-grained. We consider the various limits in which these mechanisms dominate, and compare the obtained solutions in each case so as to gain insight on the effect each mechanism has on the overall behavior of the network. This analysis is important because we know that the physical nature of the scaling solutions is highly dependent on the dominant dynamical mechanism [20].

From a physical point of view, three main scaling solution regimes are expected to exist, consisting of the Goto-Nambu solution of $\mu = 1$; a regime where wiggliness reaches

scaling, i.e., μ approaches a constant value in time $\mu = m_o$; and a regime that implies growth of small-scale structure $\mu \propto t^\gamma$. Specifically, we consider scaling solutions of the generic form

$$\begin{aligned} L &= L_o t^\alpha \\ v &= v_o t^\beta \\ \mu &= m_o t^\gamma, \end{aligned} \tag{3.1}$$

or alternatively, using Eq. (2.24):

$$\xi = L_o m_o^{1/2} t^{\alpha+\gamma/2}, \tag{3.2}$$

with $\beta \leq 0$ due to the finite speed of light, and $\alpha \leq 1$ as imposed by causality.

On a final note, it is worth having a brief discussion regarding the role of the momentum parameter k. In Minkowski space $H = 0$, one expects the VOS to hold for a null value of the momentum parameter $k = 0$ [6, 26, 27, 33]. Analogously, in an expanding universe $H \neq 0$, one expects $k \neq 0$ as confirmed by numerical simulations [26]. Having this in mind, this chapter is then organized as follows: the physically meaningful solutions are first presented, followed by a discussion of their physical implications, with the mathematical solutions of the model being treated in a separate section. Besides solutions with $k = 0 (k \neq 0)$ in expanding (non-expanding) universes, this latter category of solutions also includes ultra-relativistic solutions $v = 1$, which are not physical due to string segments having mass. Some of the results that will now be discussed have been published in Physical Review D [34].

3.1 Physical Solutions

3.1.1 No dynamical mechanisms

We start by considering the simplest case of no dynamical mechanisms acting on the network. In this case, (2.38)-(2.41) implies constant velocity and characteristic length scale of the network, either with $v = 1$ or $k = 0$. In the physically significant solution branch of

$k = 0$, these quantities are undetermined

$$\begin{aligned} L &= L_o \\ v &= v_o \\ \mu &= m_o \\ \xi &= \sqrt{m_o} L_o, \end{aligned} \tag{3.3}$$

but they could be inferred from numerical simulations. This solution depicts a network in equilibrium, in the absence of energy loss mechanisms, and thus with constant length (or equivalently, constant total energy density), as well as constant velocity and wiggliness.

3.1.2 With a running averaging scale

A few assumptions have to be made in the cases that include a coarse-graining scale. In particular, we assume the fractal dimension of Eq. (2.37) with $b = 2$ and a power-law shaped averaging scale

$$l = l_o t^{\delta}, \quad 0 < \delta \leq 1. \tag{3.4}$$

Equation (2.38) dictates that L is constant, which is no surprise because the absence of energy loss mechanisms should imply that the total energy density of the network is conserved. There are two distinct solutions in the $k = 0$ solution branch, the first being the Goto-Nambu limit

$$\begin{aligned} L &= L_o \\ v &= v_o \\ \mu &= 1 \\ \xi &= L_o, \end{aligned} \tag{3.5}$$

which is analogous to Eq.(3.3), with the difference that μ is no longer unspecified but restricted to the Goto-Nambu value. Not only do the scaling coefficients not exhibit any explicit dependence on the scale, but also this solution exists for any value of δ. This simply means that a variation in the coarse-graining scale has no influence on the evolution of the network, given that the network is devoid of small-scale structure.

The second solution found within the $k = 0$ solution branch yields

$$\begin{aligned} L &= L_o \\ v &= v_o t^{-\delta} \\ \mu &= m_o t^{\delta} \\ \xi &= \sqrt{m_o} L_o t^{\delta/2}, \end{aligned} \tag{3.6}$$

with the following constraint:

$$v_o^2 m_o^2 = 1. \tag{3.7}$$

We now find that the small-scale structure of the network is evolving in time. In the first place, we note that the domain of δ remains unrestricted, as in the previous solution Eq. (3.5), which is due to energy conservation. However, unlike what was found in Eq. (3.5), the presence of small-scale structure made this solution explicitly dependent on δ. In particular, we are always able to find small-scale structure for all choices of scale, and a variation in the scale simply changes the way energy migrates from the bare string to the wiggles, with the total energy of the network staying constant. In the second place, this growth in small-scale structure is compensated by a decrease in velocity, which seems to suggest that not only is μ scale-dependent, but v is also dependent on δ. This is in agreement with the mesoscopic velocity interpretation of the wiggly model, rather than a microscopic RMS one [19, 20].

Moreover, taking the correlation length as our scale $\ell \propto \xi$ implies

$$\delta = \frac{\delta}{2} \quad \Leftrightarrow \delta = \gamma = 0, \tag{3.8}$$

suggesting that at this scale, the only scaling regime that can exist is a constant wiggliness one. Finally, we also note that solution (3.5) can be retrieved by taking the limit $\delta \to 0$ on Eq. (3.6), discarding some slight discrepancies in the coefficients.

3.1.3 With energy losses

With the inclusion of energy loss mechanisms (specifically, the ones described by Eq. (2.34)), we find different dynamics of the network's length scales, with L and ξ now evolving in time. We determine two possible solutions in the $k = 0$ branch. The first is a

constant wiggliness solution

$$\begin{aligned} L &= L_o t \\ v &= v_o \\ \mu &= m_o \\ \xi &= \sqrt{m_o} L_o t, \end{aligned} \tag{3.9}$$

such that:

$$L_o = \frac{c v_o}{2} \frac{(1+\eta) m_o^{1/2} - \eta}{m_o} \tag{3.10}$$

$$D\left(1 - \frac{1}{m_o^2}\right) = \eta\left(1 - \frac{1}{m_o^{1/2}}\right), \quad \eta \geq D. \tag{3.11}$$

As described by the consistency relation (3.11), the small-scale structure parameters dictate which values of wiggliness are permitted, as depicted in Figure 3.1.The Goto-Nambu value is clearly a solution, but this relation includes other values of $m_o > 1$. Specifically, in the range $\frac{D}{\eta} < \frac{1}{4}$, there is only one physically meaningful solution that yields $m_o = 1$, which can be explained by the wiggliness not being able to asymptotically survive on the network when the small-scale structure that is generated makes up only a small fraction of the amount lost by the network. Conversely, for values of $\frac{D}{\eta}$ in the interval $\frac{D}{\eta} \in \left]\frac{1}{4}, 1\right[$, we find solutions with $m_o > 1$. Although this latter solution is valid from a mathematical point of view, its physical relevance is not granted for the reason that taking the limit $\eta \longrightarrow D$ on the upcoming solution, that is defined for $\eta < D$, yields $m_o \longrightarrow 1$.

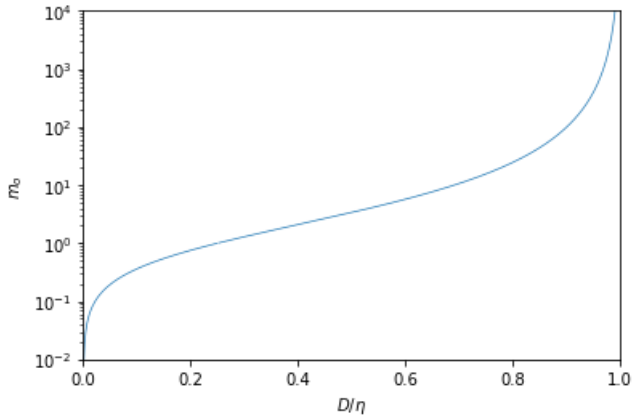

FIGURE 3.1: Dependence of the wiggliness m_o on the ratio of energy loss parameters $\frac{D}{\eta}$.

The second solution is one where small-scale structure accumulates in time

$$\begin{aligned} L &= L_o t^{\alpha} \\ v &= v_o \\ \mu &= m_o t^{2-2\alpha} \\ \xi &= \sqrt{m_o} L_o t, \end{aligned} \tag{3.12}$$

such that the following consistency relations are respected:

$$L_o = \frac{c(1+\eta)v_o}{2\alpha m_o^{1/2}}, \tag{3.13}$$

$$\alpha = \frac{1+\eta}{1+D} < 1 \tag{3.14}$$

$$\gamma = 2\frac{D-\eta}{1+D}, \quad D > \eta. \tag{3.15}$$

The set of solutions (3.9) (3.12) contain plenty of physical insight, as they allow us to infer the exact physical conditions that dictate the nature of the scaling regime. On the one hand, as seen in (3.9), when the amount of small-scale structure removed (e.g., loop production) is greater than its gain (e.g., kink formation upon intercommutation), $\eta > D$, the wiggliness of the long-strings stays constant. On the other hand, as illustrated by (3.12), when there is more production of small-scale structure on the network than loss, $D > \eta$, we find that wiggliness builds up on the long strings.

Furthermore, it should also be emphasized that while (3.9) implies that L and ξ are in linear scaling, in (3.12) we encounter different length scale dynamics, with L now scaling according to an exponent specified by the energy loss parameters, despite the correlation length maintaining its linear scaling. This is a clear illustration of the two length scale feature of the wiggly model, where each length scale has distinct dynamics. The evolution of α and γ as a function of the energy loss parameters is exhibited in Fig. 3.2.

3.1.4 With expansion

When considering expanding universes, we will always assume the scale factor takes the form of a power law

$$a = t^{\lambda}, \quad 0 < \lambda < 1. \tag{3.16}$$

The $k \neq 0$ branch yields three solution subbranches. Firstly, we find the Goto-Nambu

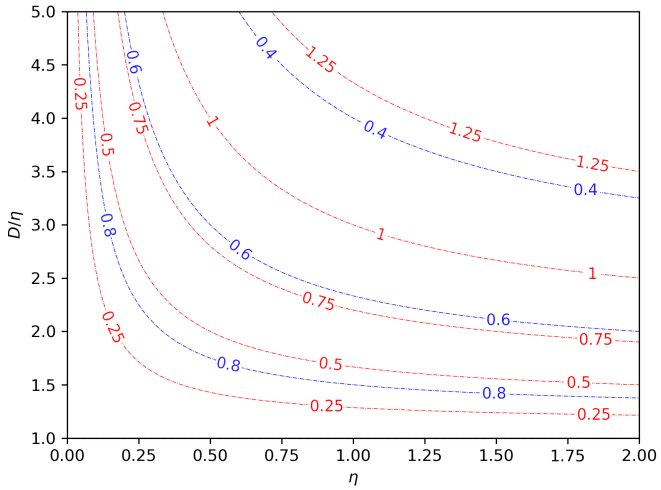

FIGURE 3.2: Scaling Exponents α (blue dashed line) and γ (red dashed line), as yielded by equations (3.14) and (3.15) respectively, as a function of parameters η and $\frac{D}{\eta}$.

solution subbranch, which has two constant velocity solutions. The ultra-relativistic solution will be addressed separately, while the non-relativistic one yields:

$$\begin{aligned} L &= \left(\frac{k^2}{4\lambda(1-\lambda)}\right)^{1/2} t \\ v &= \left(\frac{1-\lambda}{\lambda}\right)^{1/2} \\ \mu &= 1 \\ \xi &= \left(\frac{k^2}{4\lambda(1-\lambda)}\right)^{1/2} t, \end{aligned} \tag{3.17}$$

which corresponds to the canonical VOS solution (2.15). One should be mindful that not all expansion rates ensure sufficient Hubble damping in order for the network to reach linear scaling

$$v_o^2 < 1 \Leftrightarrow \lambda > \frac{1}{2}. \tag{3.18}$$

This has the implication of scaling being reachable in the matter era, but not in the radiation one, since in the latter, the network does not lose enough energy. However, interpreting this velocity as an average one imposes a different type of constraint (the value of mean velocity for loops in Minkowski space)

$$v_o^2 \leq \frac{1}{2} \Leftrightarrow \lambda \geq \frac{2}{3}. \tag{3.19}$$

Secondly, we find a solution of constant wiggliness, only viable in the matter era

$$\begin{aligned} L &= L_o t \\ v &= v_o \\ \mu &= m_o \\ \xi &= \sqrt{m_o} L \\ \lambda &= \frac{2}{3}, \end{aligned} \tag{3.20}$$

where the scaling coefficients are given by:

$$L_o = \frac{3k}{2(m_o^3 + m_o)^{1/2}}, \quad v_o = \frac{1}{(1 + m_o^2)^{1/2}}. \tag{3.21}$$

This solution illustrates the intuition hinted by Goto-Nambu numerical simulations that scaling is more easily reached in the matter era rather than in the radiation era [26]. It should also be noted that by choosing $m_o = 1$, we retrieve the previous solution (3.17). In addition, this solution allows us to draw parallels with a similar solution obtained for chiral superconducting strings [35].

Finally, we also determine a regime of small-scale structure growth, which implies decreasing velocities $\beta < 0$, and $\alpha = \frac{3}{2}\lambda$, as well as the consistency relations $\frac{3}{2}\lambda + \frac{\gamma}{2} - \beta = 1$, and $\beta + \gamma \geq 0$. Note this restricts the range of allowed expansion rates to slower rates than the matter era one $\lambda < \frac{2}{3}$. We can distinguish two regimes, depending on the value of λ. For slow expansion rates, we have

$$\begin{aligned} L &= L_o t^{3/2\lambda} \\ v &= v_o t^{-\lambda} \\ \mu &= m_o t^{2-5\lambda} \\ \xi &= \frac{v_o k}{2 - 4\lambda} t^{1-\lambda}, \end{aligned} \tag{3.22}$$

subject to the following constraints:

$$m_o = \left(\frac{v_o k}{L_o (2 - 4\lambda)} \right)^2 \tag{3.23}$$

$$\lambda \leq \frac{1}{3}. \tag{3.24}$$

In terms of the evolution of the energy density, we have that the bare string energy (normalized by the background energy density) evolves according to:

$$\frac{\rho_o}{\rho_{crit}} \propto t^{\lambda}, \tag{3.25}$$

and the total energy density of the network grows with

$$\frac{\rho}{\rho_{crit}} \propto t^{2-3\lambda}. \tag{3.26}$$

As far as the intermediate expansion rate regime is concerned, we find

$$\begin{aligned} L &= L_o t^{3/2\lambda} \\ v &= v_o t^{-\gamma} \\ \mu &= m_o t^{\gamma} \\ \xi &= \sqrt{m_o} L_o t^{\lambda+\frac{1}{3}} \\ \gamma &= \frac{2}{3} - \lambda, \end{aligned} \tag{3.27}$$

with the following constraints:

$$v_o = \frac{2}{3}\left(\frac{L_o}{(\frac{4}{3}\lambda - \frac{4}{9})^{1/4}k}\right)^{2/3}, \quad m_o = \left(\frac{k}{(\frac{4}{3}\lambda - \frac{4}{9})^{1/2}L_o}\right)^{2/3} \tag{3.28}$$

$$\lambda \in \left]\frac{1}{3}, \frac{2}{3}\right[. \tag{3.29}$$

It is worth noting that considering the limit $\lambda \longrightarrow \frac{1}{3}$, we find this solution matches the slow regime solution previously obtained. Besides this, we also recover the constant wiggliness solution (3.20) in the limit $\lambda \longrightarrow \frac{2}{3}$, apart from differences in the velocity coefficients. This scaling solution implies the following evolution of the ratio of the bare energy density

$$\frac{\rho_o}{\rho_{crit}} \propto t^{4/3-2\lambda}, \tag{3.30}$$

and of the total energy with respect to the cosmological background

$$\frac{\rho}{\rho_{crit}} \propto t^{2-3\lambda}, \tag{3.31}$$

which coincides with what was obtained for the slow expansion solution in Eq. (3.26). Furthermore, it is instructive to consider the particular case of the radiation-dominated

era ($\lambda = \frac{1}{2}$), which yields:

$$L \propto t^{3/4}, \quad v \propto t^{-1/6} \quad \mu \propto t^{1/6} \quad \xi \propto \sqrt{m_o} L_o t^{5/6}, \tag{3.32}$$

with corresponding energy density ratios:

$$\frac{\rho_{o,\mathrm{rad}}}{\rho_{crit}} \propto t^{1/3}, \quad \frac{\rho_{\mathrm{rad}}}{\rho_{crit}} \propto t^{1/2}. \tag{3.33}$$

These relations constitute an opportunity for testing with Goto-Nambu and field theory simulations.

As depicted in Fig. 3.3, greater expansion rates imply slower growth of small-scale structure. It is also worthwhile noting the distinctive dynamics yielded by the expansion rate $\lambda = \frac{1}{3}$, where we find the slowest evolution for the correlation length but the fastest velocity decay. The matter-dominated era also has interesting behavior, as it is the expansion rate for which linear scaling of the network is achievable.

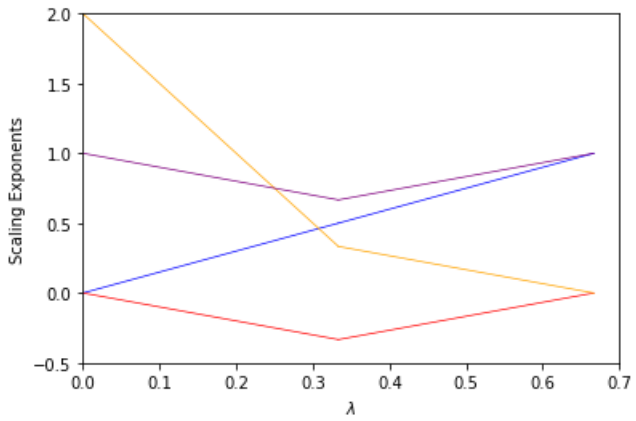

FIGURE 3.3: Scaling exponents α (blue), β (red), γ (orange) and the ξ exponent $\alpha + \frac{\gamma}{2}$, as described by equations (3.22) for slow expansion rates and (3.27) for the intermediate regime.

On a final note, analogously to what was concluded for the energy losses case in section 3.1.3, energy loss by Hubble damping also leads to a different scaling behavior for L and ξ. In both cases, for constant wiggliness, linear scaling of both L and ξ was verified. However, with the small-scale structure of the network growing in time, L now scales according to a power specified by the expansion rate and, unlike what happened in the energy loss case, the linear scaling of ξ is disrupted.

3.1.5 With energy losses and a running averaging scale

When one considers both energy losses and a running averaging scale, one finds two possible solutions.The first solution yields constant wiggliness such that:

$$\begin{aligned} L &= L_o t \\ v &= v_o \\ \mu &= 1 \\ \xi &= L, \end{aligned} \tag{3.34}$$

with the scaling coefficient for L being restricted to:

$$L_o = \frac{c(1+\eta)v_o}{2}. \tag{3.35}$$

Note this solution is analogous to Eq. (3.9), with the difference that μ is no longer an arbitrary value, but restricted to the Goto-Nambu case. We find, yet again, that in the absence of small-scale structure, a change in the coarse-graining scale does not affect the evolution of the string network.

The second solution implies growing wiggliness:

$$\begin{aligned} L &= L_o t^{\alpha} \\ v &= v_o t^{-\gamma} \\ \mu &= m_o t^{\gamma} \\ \xi &= \sqrt{m_o} L_o t^{\frac{1}{3}+\frac{2}{3}\alpha}, \end{aligned} \tag{3.36}$$

$$L_o = \frac{c(1+\eta)v_o}{2\alpha m_o^{1/2}} \tag{3.37}$$

$$\alpha = \frac{(\frac{2}{3}-\delta)(1+\eta)}{\frac{2}{3}(1+\eta)+2(D-\eta)} < 1, \quad D > \eta \tag{3.38}$$

$$\gamma = \frac{2}{3} - \frac{2}{3}\alpha = \frac{2(D-\eta)+\delta(1+\eta)}{3(D-\eta)+(1+\eta)} \tag{3.39}$$

$$\delta = \gamma v_o^2 m_o^2 \in \left]0, \frac{2}{3}\right[\tag{3.40}$$

Note that if we consider the fixed scale limit $\delta \longrightarrow 0$, we are able to recover (3.12) $\gamma \longrightarrow 0$, $\alpha \longrightarrow 1$. Additionally, we can also take the limit of no energy losses $D, \eta \to 0$ on (3.36). By doing so, we partially recover the previous solution of Eq. (3.6), namely the dynamics for the velocity and wiggliness $\gamma = -\beta = \delta$, but with distinct behavior of both the length scales.

An interesting consequence of this solution is that δ is restricted so that condition (3.40) is satisfied. The fact that the allowed averaging scale is now bounded from above is owed to the energy losses of the network. In other words, if the scale does not evolve slowly enough, we are unable to find small-scale structure.

Furthermore, we find on (3.39) that there is an explicit relation between δ and α, hinting at an apparent scale dependence of the total energy of the network. This is unexpected, as the total energy of the network should be scale-invariant. In other words, the way the network loses energy should not depend on the choice of averaging scale choice. The physics behind this behavior needs to be better understood in future studies.

Lastly, we consider a specific case study, where we choose our scale to be the correlation length $\ell \propto \xi$

$$\delta = \alpha + \frac{\gamma}{2}, \tag{3.41}$$

which yields:

$$\delta = \frac{1+D}{2(1+\eta)+3(D-\eta)} \tag{3.42}$$

$$\alpha = \frac{1}{2}\frac{(1+\eta)}{2(1+\eta)+3(D-\eta)} \tag{3.43}$$

$$\gamma = \frac{(1+\eta)+2(D-\eta)}{2(1+\eta)+3(D-\eta)} \tag{3.44}$$

$$L_o = \frac{cv_o}{m_o^{1/2}}\left(2(1+\eta)+3(D-\eta)\right) \tag{3.45}$$

$$v_o^2 m_o^2 = \frac{1+D}{(1+\eta)+2(D-\eta)}. \tag{3.46}$$

In particular, taking the limit of no energy loss $(D-\eta) \longrightarrow 0$ we find:

$$\begin{aligned} \alpha &\longrightarrow \frac{1}{4} \\ \gamma &\longrightarrow \frac{1}{2} \\ \delta &\longrightarrow \frac{1}{2} \\ v_o^2 m_o^2 &\longrightarrow 1, \end{aligned} \tag{3.47}$$

or equivalently, $L \propto t^{1/4}, \ell \propto \xi \propto \mu \propto t^{1/2}, v \propto \mu^{-1} \propto t^{-1/2}$. In an analogous manner to (3.6), we see again that the growing wiggliness is compensated by a decreasing velocity. However, there are significant differences between these two solutions. In the first place, in this solution the characteristic scale evolves in time, while the behavior of the previous solution was of a fixed characteristic scale due to the overall energy of the network being

conserved. But here, despite the absence of energy loss mechanisms, we do not retrieve $\alpha \longrightarrow 0$. Secondly, in (3.6), if one chooses the scale to be the correlation length $\ell \propto \xi$, we find that the scale is restricted to a fixed one $\delta = 0$. This is in direct contrast with the behavior depicted in this solution, where the choice of $\ell \propto \xi$ implies a time-evolving coarse-graining scale.

3.1.6 With expansion and a running averaging scale

We will consider the averaging scale formerly introduced in Eq. (3.4). Firstly, in the $k \neq 0$ solution branch we find the Goto-Nambu solution in the form

$$\begin{aligned} L &= L_o t \\ v &= v_o \\ \mu &= 1 \\ \xi &= \sqrt{m_o} L_o t \\ \lambda &> \frac{1}{2}, \end{aligned} \tag{3.48}$$

subject to the constraints

$$L_o = \left(\frac{k^2}{4\lambda(1-\lambda)} \right)^{1/2}, \quad v = \left(\frac{1-\lambda}{\lambda} \right)^{1/2}. \tag{3.49}$$

Note that the introduction of a running averaging scale neither affected the scaling behavior of previous solution (3.17), nor did it impose any restriction on δ. It should be also noted that by imposing $v_o^2 \leq \frac{1}{2}$, we derive the constraint $\lambda \geq \frac{2}{3}$.

Secondly, we found one solution of non-trivial constant wiggliness and constant velocity

$$\begin{aligned} L &= L_o t \\ v &= v_o \\ \mu &= m_o \\ \xi &= \sqrt{m_o} L_o t \\ \lambda &< \frac{2}{3} \end{aligned} \tag{3.50}$$

$$v_o = \left(\frac{1 + m_o^2(2\lambda^{-1} - 3)}{1 + m_o^2} \right)^{1/2} \tag{3.51}$$

$$\delta = (1 - \frac{3}{2}\lambda) m_o^2 (1 + m_o^2). \tag{3.52}$$

This solution makes it evident that the inclusion of a renormalization scale decreased the value of the expansion rate for which full scaling regime takes place, being now achieved for expansion rates lower than the matter era one.

Choosing $\ell \propto \xi$, we find

$$\delta = 1, \tag{3.53}$$

and consequently

$$\frac{1}{1-\frac{3}{2}\lambda} = m_o^2(1+m_o^2). \tag{3.54}$$

Lastly, we find various solutions with growing small-scale structure, which entail the same dynamics for the characteristic length scale and velocity as found for the expansion case (section 3.1.4), namely $\alpha = \frac{3}{2}\lambda$, $\beta < 0$, and $\frac{3}{2}\lambda + \frac{\gamma}{2} - \beta = 1$, and $\beta + \gamma \geq 0$. The first one is defined for slow expansion rates and is a generalization of (3.22), such that in the limit $\delta \to 0$, we recover this previous solution:

$$\begin{aligned} L &= L_o t^{3/2\lambda} \\ v &= v_o t^{-\lambda} \\ \mu &= m_o t^{2-5\lambda} \\ \xi &= \sqrt{m_o} L_o t^{1-\lambda} \\ \lambda &\leq \frac{1}{3}, \end{aligned} \tag{3.55}$$

where the scaling coefficients are related by:

$$m_o = \left(\frac{k v_o}{L_o(2-4\lambda+\delta)} \right)^2. \tag{3.56}$$

In particular, if we choose our scale to be the correlation length of the network $\ell \propto \xi$ we get

$$\delta = 1 - \lambda \tag{3.57}$$

$$m_o = \left(\frac{k v_o}{L_o(3-5\lambda)} \right)^2. \tag{3.58}$$

Lastly, for intermediate expansion rates we find:

$$\begin{aligned} L &= L_o t^{3/2\lambda} \\ v &= v_o t^{-\gamma} \\ \mu &= m_o t^{\gamma} \\ \xi &= \sqrt{m_o} L_o t^{1/3+\lambda} \\ \frac{1}{3} &< \lambda < \frac{2}{3}, \end{aligned} \tag{3.59}$$

such that

$$v_o = \left(\frac{1}{(3\lambda - 1) m_o^2} \right)^{1/2}, \quad m_o = \left(\frac{k v_o}{L_o (\frac{2}{3} + \delta)} \right)^2 \tag{3.60}$$

$$\gamma = \frac{2}{3} - \lambda. \tag{3.61}$$

Again, choosing $\ell \propto \xi$ we determine:

$$\delta = \frac{1}{3} + \lambda \tag{3.62}$$

$$m_o = \left(\frac{k v_o}{L_o (1 + \lambda)} \right)^2. \tag{3.63}$$

Note that these solutions match for an expansion rate $\lambda = \frac{1}{3}$.

3.1.7 With expansion and energy losses

We now consider the case of a network subject to energy losses in an expanding universe. We find three solutions regimes. Firstly, in the Goto-Nambu subbranch we find:

$$\begin{aligned} L &= L_o t \\ v &= v_o \\ \mu &= 1 \\ \xi &= L_o t, \end{aligned} \tag{3.64}$$

with the following scaling coefficients:

$$L_o = \left(\frac{k(k+c)}{4\lambda(1-\lambda)} \right)^{1/2}, \quad v = \left(\frac{k(1-\lambda)}{\lambda(k+c)} \right)^{1/2}. \tag{3.65}$$

which corresponds to the well-known scale-invariant solution of the VOS (2.15). Note that (3.17) is a particular case of (3.64) for which $c = 0$. The physical implication of this

is that there are cases where the network's intrinsic energy losses are not needed for the network to reach linear scaling, since Hubble damping is enough to ensure this.

Secondly, we find a full scaling solution

$$\begin{aligned} L &= L_o t \\ v &= v_o \\ \mu &= m_o \\ \xi &= \frac{k}{\lambda v_o (1+m_o^2)} t, \end{aligned} \tag{3.66}$$

subject to the following constraint relations

$$L_o^2 = \frac{k}{\lambda} \frac{k + c(1+\eta)m_o^2 - c\eta m_o^{3/2}}{m_o(1+m_o^2)(\lambda + (2-3\lambda)m_o^2)} \tag{3.67}$$

$$v_o^2 = \frac{k}{\lambda} \frac{\lambda + (2-3\lambda)m_o^2}{(1+m_o^2)(k + c(1+\eta)m_o^2 - c\eta m_o^{3/2})} \tag{3.68}$$

$$\left(\lambda + m_o^2(2-3\lambda)\right)\left((k+cD)(1-\frac{1}{m_o^2}) - c\eta(1-\frac{1}{m_o^{1/2}})\right) = \lambda\left(1-\frac{1}{m_o^2}\right)\left(k + (1+\eta-\eta m_o^{-1/2})m_o^2 c\right). \tag{3.69}$$

We point out that the previous solution (3.20) is retrieved by direct substitution of $\lambda = \frac{2}{3}$, and $c = 0$ on this solution. In order to gain more insight into this solution, we consider two case studies of small and great amounts of wiggliness. In the small wiggliness limit, we can do a Taylor series expansion, defining

$$m_o \sim 1 + y_o, \tag{3.70}$$

where y is a first-order correction to the Goto-Nambu solution. It follows that the normalization coefficients of (3.67) (3.68) become

$$L_o^2 = L_{GN}^2 \left(1 + \left(\frac{c}{k+c}(2+\frac{1}{2}\eta) + \frac{5\lambda-4}{1-\lambda}\right) y_o\right) \tag{3.71}$$

$$v_o^2 = v_{GN}^2 \left(1 + \left(\frac{1-2\lambda}{1-\lambda} - \frac{c}{k+c}(2+\frac{1}{2}\eta)\right) y_o\right), \tag{3.72}$$

with y_o being given by

$$y_o = \frac{\lambda(k+c) + (\lambda-1)(2(k+cD) - c\eta/2)}{(2-3\lambda)(2(k+cD) - c\eta/2) - c\lambda(2+\eta/2)}. \tag{3.73}$$

Before considering the limit of large wiggliness, we define new parameters

$$\begin{aligned} k_{eff} &\equiv k + c(D - \eta) \\ c_{eff} &\equiv c(1 + \eta). \end{aligned} \tag{3.74}$$

These definitions carry physical meaning, as the existence of small-scale structure on the network modifies string curvature and further stimulates energy losses. The large wiggliness limit

$$m_o \gg 1, \tag{3.75}$$

yields:

$$\begin{aligned} L_o &= \left(\frac{k c_{eff}}{\lambda m_o^3 (2 - 3\lambda)} \right)^{1/2} \\ v_o &= \left(\frac{k(2 - 3\lambda)}{\lambda m_o^2 c_{eff}} \right)^{1/2} \\ \lambda &= \frac{2k_{eff}}{c_{eff} + 3k_{eff}}, \end{aligned} \tag{3.76}$$

which demonstrates how, when there are great amounts of wiggliness on the network, the overall energy density increases while the velocity decreases, as one would predict. In addition, it is also interesting to note that in the radiation era, the effective parameters become equal

$$k_{eff} = c_{eff}. \tag{3.77}$$

This relation provides a way for testing with numerical simulations.

Thirdly, we find solutions of growing wiggliness. Analogously to the expanding case, we find the same implication of $\beta < 0$, although $\alpha = \frac{3}{2}\lambda$ does no longer hold, and instead we have $\alpha > \frac{3}{2}\lambda$. Physically, this is expected since the inclusion of energy losses implies faster energy loss. We again differentiate solutions depending on the expansion rate. For slow expansion rates, we find

$$\begin{aligned} L &= L_o t^{\alpha} \\ v &= v_o t^{-\lambda} \\ \mu &= m_o t^{\gamma} \\ \xi &= \sqrt{m_o} L_o t^{1-\lambda}, \end{aligned} \tag{3.78}$$

with the following consistency conditions:

$$\alpha = \frac{1}{2} \frac{2c_{eff} + \lambda(3k_{eff} - c_{eff})}{k_{eff} + c_{eff}} \tag{3.79}$$

$$\gamma = 2 - 2\lambda - 2\alpha = \frac{2k_{eff} - \lambda(c_{eff} + 5k_{eff})}{k_{eff} + c_{eff}} \tag{3.80}$$

$$\gamma \in]0, 2 - 5\lambda[\tag{3.81}$$

$$\lambda \leq \frac{k_{eff}}{3k_{eff} + c_{eff}}. \tag{3.82}$$

It is worth pointing out that one obtains the previous slow expansion solution (3.22) in the limit $c \longrightarrow 0$. This solution implies that the ratio of bare string energy in relation to the background energy density has an evolution given by:

$$\frac{\rho_o}{\rho_{crit}} \propto t^{2\lambda}, \tag{3.83}$$

while the total energy density of the network grows according to

$$\frac{\rho}{\rho_{crit}} \propto t^{2\lambda+\gamma}. \tag{3.84}$$

In the intermediate expansion rate regime, we find:

$$\begin{aligned} L &= L_o t^{\alpha} \\ v &= v_o t^{-\gamma} \\ \mu &= m_o t^{\gamma} \\ \xi &= \sqrt{m_o} L_o t^{\frac{1}{3}+\frac{2}{3}\alpha} \end{aligned} \tag{3.85}$$

$$L_o^2 = \frac{k c_{eff}}{(2\alpha - 3\lambda)(\lambda + \frac{2}{3}\alpha - \frac{2}{3})m_o^3} \tag{3.86}$$

$$v_o^2 = \frac{k(2\alpha - 3\lambda)}{c_{eff}(\lambda + \frac{2}{3}\alpha - \frac{2}{3})m_o^2} \tag{3.87}$$

$$\alpha = \frac{\frac{2}{3}c_{eff} + \lambda(3k_{eff} + c_{eff})}{\frac{2}{3}c_{eff} + 2k_{eff}} \tag{3.88}$$

$$\gamma = \frac{2}{3} - \frac{2}{3}\alpha = \frac{2k_{eff} - \lambda(3k_{eff} + c_{eff})}{c_{eff} + 3k_{eff}} \tag{3.89}$$

$$\lambda \in \left] \frac{k_{eff}}{3k_{eff} + c_{eff}}, \frac{2k_{eff}}{3k_{eff} + c_{eff}} \right[. \tag{3.90}$$

Analogously to the slow expansion case, one is also able to retrieve the previous solution Eq. (3.27) in the limit $c \to 0$. It should also be emphasized that the domain of the expansion rate parameter changed to a broader one, when in comparison to (3.27), which can be attributed to now there being two mechanics by which the network can lose energy, not just by Hubble damping. For the intermediate regime, the evolution of the network's

energy densities is described by:

$$\frac{\rho_o}{\rho_{crit}} \propto t^{2\gamma} \tag{3.91}$$

$$\frac{\rho}{\rho_{crit}} \propto t^{3\gamma}. \tag{3.92}$$

An interesting consequence of this set of solutions comes from noting that the two regimes match for the expansion rate given by

$$\lambda = \frac{k_{eff}}{3k_{eff} + c_{eff}}, \tag{3.93}$$

which is half of the expansion rate of (3.76). The dependence of this expansion rate on the effective parameters is shown in Fig. 3.4. We also point out that in the limit $c \longrightarrow 0$, (3.93) approaches $\lambda \longrightarrow \frac{1}{3}$.

On a last note, it is also interesting to consider the particular case where the effective curvature balances out the looping chop parameter

$$k_{eff} = c_{eff}, \tag{3.94}$$

which yields the following scaling solution in the slow regime

$$\begin{aligned} \alpha_{slow} &= \frac{1+\lambda}{2} \\ \gamma_{slow} &= 1 - 3\lambda \\ \lambda &\leq \frac{1}{4}, \end{aligned} \tag{3.95}$$

while in the intermediate regime we find:

$$\begin{aligned} \alpha_{int} &= \frac{1}{4} + \frac{3}{2}\lambda \\ \gamma_{int} &= \frac{1}{2} - \lambda \\ \lambda &\in \left]\frac{1}{4}, \frac{1}{2}\right[. \end{aligned} \tag{3.96}$$

As concluded before in (3.77), the radiation era enables the network to reach full scaling $\alpha = 1, \gamma = 0$ under the condition of $k_{eff} = c_{eff}$.

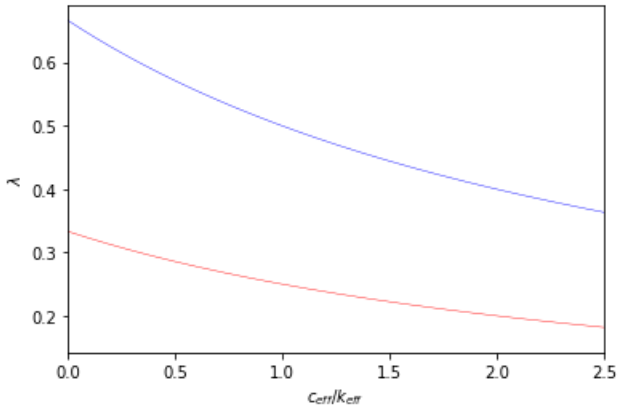

FIGURE 3.4: The expansion rate for which the transition between slow and intermediate regimes occurs in growing wiggliness solutions, given by Eq. (3.93), as a function of the ratio $\frac{c_eff}{k_eff}$ (red solid line), and the transition rate for the full linear scaling solution as yielded by (3.76), represented by the blue line.

3.1.8 With expansion, energy losses and a running averaging scale

At last, we consider the most realistic case that includes all the three dynamical mechanisms. In this case, the three scaling regimes are predicted to exist. Firstly, in the Goto-Nambu solution branch, we obtain the previous VOS solution

$$\begin{aligned} L &= L_o t \\ v &= v_o \\ \mu &= 1 \\ \xi &= L_o t, \end{aligned} \tag{3.97}$$

with the following scaling coefficients:

$$L_o = \left(\frac{k(k+c)}{4\lambda(1-\lambda)}\right)^{1/2}, \quad v = \left(\frac{k(1-\lambda)}{\lambda(k+c)}\right)^{1/2}. \tag{3.98}$$

Secondly, we find a full linear scaling solution

$$\begin{aligned} L &= L_o t \\ v &= v_o \\ \mu &= m_o \\ \xi &= \sqrt{m_o} L_o t, \end{aligned} \tag{3.99}$$

subject to the following consistency relations:

$$L_o^2 = \frac{\left(c\eta m_o^{3/2} - c(1+\eta)m_o^2\right)\left(\delta(1-m_o^{-2})(c(1+\eta)m_o^4 - c\eta m_o^{7/2} + km_o^2) - k(1+m_o^2)(\lambda + (2-3\lambda)m_o^2)\right) + }{\lambda m_o\left(\delta(m_o^2-1) + (m_o^2+1)(\lambda + (2-3\lambda)m_o^2)\right)^2}$$
$$\frac{k^2(m_o^2+1)\left(\lambda + (2-3\lambda)m_o^2\right)}{\lambda m_o\left(\delta(m_o^2-1) + (m_o^2+1)(\lambda + (2-3\lambda)m_o^2)\right)^2} \tag{3.100}$$

$$v_o^2 = \frac{\delta(1-m_o^{-2})\left(c\eta m_o^{7/2} - c(1+\eta)m_o^4\right) + k(m_o^2+1)\left(\lambda + (2-3\lambda)m_o^2\right)}{\lambda(1+m_o^2)\left[k(m_o^2+1) + (m_o^{-2}+1)(c(1+\eta)m_o^4 - c\eta m_o^{7/2})\right]} \tag{3.101}$$

$$\begin{aligned}
&\lambda\left(1-\frac{1}{m_o^2}\right)\left(k(m_o^2+1) + (m_o^{-2}+1)(c(1+\eta)m_o^4 - c\eta m_o^{7/2})\right)\\
&-\delta\left(1-\frac{1}{m_o^2}\right)\left(c(1+\eta)m_o^4 + (2k+c+cD)m_o^2 - c\eta m_o^{7/2} - cD\right)\\
&= \left(\lambda + m_o^2(2-3\lambda)\right)(1+m_o^2)\left((k+cD)(1-\frac{1}{m_o^2}) - c\eta(1-\frac{1}{m_o^{1/2}})\right),
\end{aligned} \tag{3.102}$$

which simplifies to Eq. (3.66) in the limit $\delta \to 0$.

Finally, we obtain solutions that imply small-scale structure growth. In the slow expansion regime we find:

$$\begin{aligned}
L &= L_o t^{\alpha}\\
v &= v_o t^{-\lambda}\\
\mu &= m_o t^{2-2(\alpha+\lambda)}\\
\xi &= \sqrt{m_o} L_o t^{1-\lambda},
\end{aligned} \tag{3.103}$$

$$L_o m_o^{1/2} = \frac{c(1+\eta)v_o}{(2\alpha - 3\lambda)} \tag{3.104}$$

$$\alpha = \frac{1}{2}\frac{(2-\delta)c_{eff} + \lambda(3k_{eff} - c_{eff})}{k_{eff} + c_{eff}} < 1 \tag{3.105}$$

$$\gamma = 2(1-\lambda-\alpha) = \frac{\delta c_{eff} + 2k_{eff} - \lambda(c_{eff} + 5k_{eff})}{k_{eff} + c_{eff}} \tag{3.106}$$

$$\lambda \leq \frac{1}{2}\frac{2k_{eff} + \delta c_{eff}}{3k_{eff} + c_{eff}}, \tag{3.107}$$

which simplifies to Eq. (3.78) in the fixed scale limit $\delta \to 0$. Furthermore, eliminating energy losses by Hubble damping $\lambda \longrightarrow 0$ yields the previous solution (3.12). It can also

be concluded that the evolution of both the total energy of the network and the bare string energy is not altered by the introduction of the averaging scale as we recover what was obtained in (3.83) (3.84).

$$\frac{\rho_o}{\rho_{crit}} \propto t^{2\lambda} \tag{3.108}$$

$$\frac{\rho}{\rho_{crit}} \propto t^{2\lambda+\gamma}. \tag{3.109}$$

Choosing the renormalization scale to be the correlation length $\ell \propto \xi$:

$$L = L_o t^{\alpha}, \quad v = v_o t^{-\lambda}, \quad \mu = m_o t^{2-2(\alpha+\lambda)}, \quad \xi = \sqrt{m_o} L_o t^{1-\lambda} \tag{3.110}$$

$$L_o m_o^{1/2} = \frac{c(1+\eta)v_o}{(2\alpha - 3\lambda)} \tag{3.111}$$

$$\alpha = \frac{1}{2}\frac{c_{eff} + 3k_{eff}\lambda}{k_{eff} + c_{eff}} \tag{3.112}$$

$$\gamma = \frac{2k_{eff} + c_{eff} - \lambda(2c_{eff} + 5k_{eff})}{k_{eff} + c_{eff}} \tag{3.113}$$

$$\lambda \leq \frac{2k_{eff} + c_{eff}}{6k_{eff} + 3c_{eff}}. \tag{3.114}$$

For intermediate expansion rates, we have

$$\begin{aligned} L &= L_o t^{\alpha} \\ v &= v_o t^{-\gamma} \\ \mu &= m_o t^{\gamma} \\ \xi &= \sqrt{m_o} L_o t^{\frac{1}{3}+\frac{2}{3}\alpha}, \end{aligned} \tag{3.115}$$

$$L_o = \frac{c_{eff} v_o}{(2\alpha - 3\lambda) m_o^{1/2}} \tag{3.116}$$

$$\alpha = \frac{(\frac{2}{3} - \delta)c_{eff} + \lambda(3k_{eff} + c_{eff})}{\frac{2}{3}c_{eff} + 2k_{eff}} < 1 \tag{3.117}$$

$$\gamma = \frac{2}{3} - \frac{2}{3}\alpha = \frac{c_{eff}\delta + 2k_{eff} - \lambda(3k_{eff} + c_{eff})}{c_{eff} + 3k_{eff}} \tag{3.118}$$

$$\delta = \alpha\left(\frac{2k}{c_{eff}} - \frac{2}{3}v_o^2 m_o^2\right) - \lambda\left(\frac{3k}{c_{eff}} + v_o^2 m_o^2\right) + \frac{2}{3}v_o^2 m_o^2. \tag{3.119}$$

$$\lambda \in \left]\frac{1}{2}\frac{2k_{eff} + \delta c_{eff}}{3k_{eff} + c_{eff}}, \frac{2k_{eff} + \delta c_{eff}}{3k_{eff} + c_{eff}}\right[. \tag{3.120}$$

It should be noted that in the fixed scale limit $\delta \longrightarrow 0$, we retrieve the previous solution (3.85). In addition, in the no expansion limit $\lambda \longrightarrow 0$, we obtain the exact coefficients

of Eq. (3.36). We also recover the same evolution of the network's associated energy densities as in (3.91) (3.92)

$$\frac{\rho_o}{\rho_{crit}} \propto t^{2\gamma} \tag{3.121}$$

$$\frac{\rho}{\rho_{crit}} \propto t^{3\gamma}. \tag{3.122}$$

Choosing $\ell \propto \xi$:

$$L = L_o t^{\alpha}, \quad v = v_o t^{-\gamma}, \quad \mu = m_o t^{\gamma} \quad \xi = \sqrt{m_o} L_o t^{\frac{1}{3}+\frac{2}{3}\alpha} \tag{3.123}$$

$$L_o = \frac{c_{eff} v_o}{(2\alpha - 3\lambda) m_o^{1/2}} \tag{3.124}$$

$$\alpha = \frac{\frac{1}{2}c_{eff}k_{eff} - \frac{1}{6}c_{eff}^2 + \frac{3}{2}\lambda(3k_{eff}^2 + k_{eff}c_{eff})}{\frac{1}{3}c_{eff}^2 + 2k_{eff}c_{eff} + 3k_{eff}^2} \tag{3.125}$$

$$\gamma = \frac{c_{eff}k_{eff} + \frac{1}{9}c_{eff}^2 + 2k_{eff}^2 - \lambda(3k_{eff}^2 + k_{eff}c_{eff})}{\frac{1}{3}c_{eff}^2 + 2k_{eff}c_{eff} + 3k_{eff}^2} \tag{3.126}$$

Finally, we also study the case where the effective curvature matches the looping chop parameter

$$k_{eff} = c_{eff}, \tag{3.127}$$

which yields in the slow regime

$$\begin{aligned} \alpha_{slow} &= \frac{(1-\frac{\delta}{2}) + \lambda}{2} \\ \gamma_{slow} &= 1 + \frac{\delta}{2} - 3\lambda \\ \lambda &\leq \frac{1+\delta}{4}, \end{aligned} \tag{3.128}$$

while in the intermediate regime we find:

$$\begin{aligned} \alpha_{int} &= \left(\frac{1}{4} - \frac{3}{8}\delta\right) + \frac{3}{2}\lambda \\ \gamma_{int} &= \frac{\delta}{4} + \frac{1}{2} - \lambda \\ \lambda &\in \left]\frac{1+\delta}{4}, \frac{1+\frac{\delta}{2}}{2}\right[. \end{aligned} \tag{3.129}$$

Linear scaling of the network can be reached under the condition

$$\lambda = \frac{1}{2} + \frac{\delta}{4}. \tag{3.130}$$

3.2 Mathematical Solutions

For the sake of completeness, we also include the mathematical allowed solutions of the wiggly model, that had no relevance for the physical analysis that was the purpose of the previous section. These include ultra-relativistic solutions, as well as solutions for $k = 0$ ($k \neq 0$) in expanding (non-expanding) universes.

3.2.1 No dynamical mechanisms

In the absence of mechanisms acting on the network, it had already been established that the length scale and velocity of the network are constant, either with $k = 0$ or $v = 1$. In the ultra-relativistic solution branch, one finds the Goto-Nambu solution

$$\begin{aligned} L &= L_o \\ v &= 1 \\ \mu &= 1 \\ \xi &= L \end{aligned} \tag{3.131}$$

and a solution where the renormalized string mass scales according to a quadratic power, thus implying linear scaling of the correlation length

$$\begin{aligned} L &= L_o \\ v &= 1 \\ \mu &= \left(\frac{k}{2L_o}\right)^2 t^2 \\ \xi &= \frac{k}{2}t. \end{aligned} \tag{3.132}$$

This growth of wiggliness, in spite of the absence of physical mechanisms, is owed to the effect of local curvature of strings segments, quantified by the momentum parameter k.

3.2.2 With a running averaging scale

We consider the same assumptions regarding the averaging scale as in section 3.1.2. In this case, we again find two possible branches of solutions. The first solution branch entails $\gamma = 0$, either with $m_o = 1$ or $m_o > 1$. This latter subbranch implies $k = 0$ which was previously explored in section 3.1.2. The other subbranch implies ultra-relativistic

velocities:

$$\begin{aligned} L &= L_o \\ v &= 1 \\ \mu &= 1 \\ \xi &= L \end{aligned} \tag{3.133}$$

In the second solution branch, one necessarily has $1+\beta-\frac{\gamma}{2}=0$. There is a constant velocity solution that either imposes $v=1$ or $\delta=1$:

$$\begin{aligned} L &= L_o \\ v &= v_o \\ \mu &= \left(\frac{kv_o}{(2-\delta)L_o}\right)^2 t^2 \\ \xi &= \frac{kv_o}{2-\delta}t \end{aligned} \tag{3.134}$$

$$\delta = 1 \quad \vee \quad v = 1. \tag{3.135}$$

By direct comparison of (3.134) with (3.132), it is clear that the introduction of an averaging scale forces the renormalized string mass to be scale dependent, despite not breaking its quadratic scaling. In particular, μ increases with δ for $\delta<2$, but decreases for $\delta>2$, being undefined at $\delta=\gamma=2$. In addition, there is also a freezing solution

$$\begin{aligned} L &= L_o \\ v &= v_o t^{-2/3} \\ \mu &= m_o t^{2/3} \\ \xi &= \sqrt{m_o} L_o t^{1/3} \end{aligned} \tag{3.136}$$

$$v_o = \left(\frac{L_o(\frac{2}{3}-\delta)(3\delta-1)^{1/4}}{k}\right)^{2/3}, \quad m_o = \left(\frac{k(3\delta-1)^{1/2}}{L_o(\frac{2}{3}-\delta)}\right)^{2/3}, \tag{3.137}$$

which, analogously to solution (3.6), is a clear depiction of the mesoscopic interpretation of the velocity. It should be noted that if one takes the coarse-graining scale to be the correlation length $\ell \propto \xi$, one finds the solution is undefined at this scale:

$$\delta = \frac{1}{3} \quad \Rightarrow v_o = m_o = 0. \tag{3.138}$$

3.2.3 With energy losses

If one assumes the energy loss terms given by (2.34), one finds two possible ultra-relativistic solutions. On the one hand, there is a full linear scaling solution

$$\begin{aligned} L &= L_o t \\ v &= 1 \\ \mu &= m_o \\ \xi &= \sqrt{m_o} L, \end{aligned} \tag{3.139}$$

such that:

$$L_o = \frac{c}{2}\frac{(1+\eta)m_o^{1/2} - \eta}{m_o} \tag{3.140}$$

$$(k + cD)\left(1 - \frac{1}{m_o^2}\right) = c\eta\left(1 - \frac{1}{m_o^{1/2}}\right). \tag{3.141}$$

Note this allows for a wide range of non-trivial wiggliness values, besides the Goto-Nambu solution $m_o = 1$ for which the solution becomes:

$$\begin{aligned} L &= \frac{c}{2} t \\ v &= 1 \\ \mu &= 1 \\ \xi &= L. \end{aligned} \tag{3.142}$$

On the other hand, a small-scale structure growth solution is also possible:

$$\begin{aligned} L &= L_o t^{\alpha} \\ v &= v_o \\ \mu &= m_o t^{2-2\alpha} \\ \xi &= \sqrt{m_o} L_o, \end{aligned} \tag{3.143}$$

$$m_o = \left(\frac{v_o(k + c(1+D))}{2L_o}\right)^2 \tag{3.144}$$

$$\alpha = \frac{c(1+\eta)}{k + c(1+D)} < 1 \tag{3.145}$$

$$\gamma = 2\frac{k + c(D-\eta)}{k + c(1+D)}, \quad D > \eta - \frac{k}{c}. \tag{3.146}$$

It is worth noting that the conditions behind each scaling regime that were derived here are analogous to the ones obtained in Eq. (3.9) (3.12). On the one hand, in (3.139),

$D < \eta - \frac{k}{c}$ implies the wiggliness on the long-strings remains constant. On the other hand, in (3.143), the small-scale structure parameters obey $D > \eta - \frac{k}{c}$, thus enabling small-scale structure to grow. It should also be pointed out that we arrive at the same conclusions as in the $k = 0$ branch, namely, the energy loss mechanism modified the scaling behavior, forcing the characteristic lengthscale L and the correlation length ξ to scale; and the correlation length maintains its linear scaling, independently of small-scale structure build-up.

3.2.4 With expansion

As before, we consider power-law expanding universes. Firstly, we find the Goto-Nambu solution. In the $k = 0$ subbranch, this yields a decreasing velocity solution

$$\begin{aligned} L &= L_o t^{\lambda} \\ v &= v_o t^{-2\lambda} \\ \mu &= 1 \\ \xi &= L, \end{aligned} \tag{3.147}$$

while in the ultra-relativistic subbranch we obtain:

$$\begin{aligned} L &= L_o t^{2\lambda} \\ v &= 1 \\ \mu &= 1 \\ \xi &= L \\ \lambda &< \frac{1}{2}. \end{aligned} \tag{3.148}$$

For $k = 0$ we find that no other regimes are possible, whereas for $v = 1$ we find a constant wiggliness solution

$$\begin{aligned} L &= L_o t \\ v &= 1 \\ \mu &= \left(\frac{2k}{L_o}\right)^2 \\ \xi &= 2kt \\ \lambda &= \frac{1}{2}, \end{aligned} \tag{3.149}$$

as well as a growing wiggliness solution:

$$\begin{aligned} L &= L_o t^{2\lambda} \\ v &= 1 \\ \mu &= \left(\frac{k}{L_o(2-3\lambda)}\right)^2 t^{2-4\lambda} \\ \xi &= \frac{k}{2-3\lambda} t \\ \lambda &< \frac{1}{2}. \end{aligned} \tag{3.150}$$

3.2.5 With energy losses and a running averaging scale

Allowing for energy losses and a varying scale, we find that the three scaling regimes are possible. The Goto-Nambu regime, as well as the constant wiggliness one, requires $v = 1$:

$$\begin{aligned} L &= \frac{c}{2} t \\ v &= 1 \\ \mu &= 1 \\ \xi &= L, \end{aligned} \tag{3.151}$$

which corresponds to the previously obtained solution of Eq. (3.142), implying that the introduction of a renormalization scale did not modify its scaling coefficients or the linear scaling of both length scales. The regime where the wiggliness is in scaling yields:

$$\begin{aligned} L &= L_o t \\ v &= 1 \\ \mu &= m_o \\ \xi &= L \end{aligned} \tag{3.152}$$

$$L_o = \frac{c}{2} \frac{(1+\eta) m_o^{1/2} - \eta}{m_o} \tag{3.153}$$

$$c\eta(2-\delta) + \frac{\delta c \eta}{m_o^2} - \frac{2(k+cD) + \delta c(1+\eta)}{m_o^{3/2}} + \left(\delta c(1+\eta) - 2(c\eta - (k+cD))\right) m_o^{1/2} = 0. \tag{3.154}$$

Note that this solution matches that of Eq. (3.139) in the fixed scale limit $\delta \longrightarrow 0$. The introduction of the averaging scale simply modified the allowed values for the wiggliness, which are now dictated by Eq. (3.154).

Moreover, two possible growing wiggliness solutions exist for $k \neq 0$

$$\begin{aligned} L &= L_o t^{\alpha} \\ v &= v_o \\ \mu &= m_o t^{2-2\alpha} \\ \xi &= \sqrt{m_o} L_o t \end{aligned} \tag{3.155}$$

$$L_o = \frac{c v_o (1+\eta)}{2\alpha m_o^{1/2}} \tag{3.156}$$

$$\alpha = \frac{1}{2}\frac{(2-\delta)c(1+\eta)}{k + c(1+D)} < 1 \tag{3.157}$$

$$\gamma = \frac{2k + 2c(D-\eta) + \delta c(1+\eta)}{k + c(1+D)}, \tag{3.158}$$

which yields solution Eq. (3.143) in the fixed scale limit $\delta \longrightarrow 0$. This solution has two possible bifurcations: one that implies $v = 1$, and another that specifies δ (and consequently, α)

$$v = 1 \vee \delta = \frac{2k}{3k + 2c(1+D)}, \alpha = \frac{2c(1+\eta)}{3k + 2c(1+D)} \tag{3.159}$$

The other growing wiggliness solution yields:

$$\begin{aligned} L &= L_o t^{\alpha} \\ v &= v_o t^{-\gamma} \\ \mu &= m_o t^{\gamma} \\ \xi &= \sqrt{m_o} L_o t^{\frac{1}{3}+\frac{2}{3}\alpha} \end{aligned} \tag{3.160}$$

$$L_o = \frac{c(1+\eta)v_o}{2\alpha m_o^{1/2}} \tag{3.161}$$

$$\alpha = \frac{(\frac{2}{3}-\delta)c(1+\eta)}{\frac{2}{3}c(1+\eta) + 2(k + c(D-\eta))} < 1 \tag{3.162}$$

$$\gamma = \frac{2}{3} - \frac{2}{3}\alpha = \frac{2(k + c(D-\eta)) + \delta c(1+\eta)}{c(1+\eta) + 3(k + c(D-\eta))} \tag{3.163}$$

$$\delta = \alpha\left(\frac{2k}{c(1+\eta)} - \frac{2}{3}v_o^2 m_o^2\right) + \frac{2}{3}v_o^2 m_o^2. \tag{3.164}$$

We again conclude that the allowed averaging scale is restricted due to the network losing energy, with δ explicitly depending on the loop chopping parameter c and the small-scale structure loss parameter η. In addition, the unexpected dependence of α on δ is also a requirement of this solution, implying that the way the network loses energy depends on

the choice of averaging scale.

3.2.6 With expansion and a running averaging scale

Accounting for expansion and a varying renormalization scale, one finds that the Goto-Nambu solution $m_o = 1$ is only possible requiring $v = 1$:

$$\begin{aligned} L &= L_o t^{2\lambda} \\ v &= 1 \\ \mu &= 1 \\ \xi &= L \\ \lambda &< \frac{1}{2}. \end{aligned} \tag{3.165}$$

In the radiation era, there is a full scaling solution

$$\begin{aligned} L &= L_o t \\ v &= 1 \\ \mu &= m_o \\ \xi &= \sqrt{m_o} L_o t \\ \lambda &= \frac{1}{2} \end{aligned} \tag{3.166}$$

$$\left(\frac{1}{2} - \delta\right) m_o^{1/2} + \left(\delta - \frac{1}{2}\right) m_o^{5/2} + \frac{k}{L_o} m_o^2 - \frac{k}{L_o} = 0. \tag{3.167}$$

Finally, there is also a solution that implies small-scale structure growth

$$\begin{aligned} L &= L_o t^{2\lambda} \\ v &= 1 \\ \mu &= \left(\frac{k}{L_o(2 - 3\lambda - \delta)}\right)^2 t^{2-4\lambda} \\ \xi &= \frac{k}{2 - 3\lambda - \delta} t \\ \lambda &< \frac{1}{2} \\ \delta &< 2 - 3\lambda, \end{aligned} \tag{3.168}$$

which in the limit $\delta \longrightarrow 0$ simplifies to (3.150).

3.2.7 With expansion and energy losses

We start by noting that in the $k = 0$ solution branch, the Goto-Nambu solution is only possible for $v = 1$

$$\begin{aligned} L &= L_o t^{2\lambda} \\ v &= 1 \\ \mu &= 1 \\ \xi &= L \\ \lambda &< \frac{1}{2}. \end{aligned} \tag{3.169}$$

Besides this, one can also find the Goto-Nambu limit for $v = 1$ and $k \neq 0$

$$\begin{aligned} L &= \frac{c}{2-4\lambda} t \\ v &= 1 \\ \mu &= 1 \\ \xi &= L \\ \lambda &< \frac{1}{2}. \end{aligned} \tag{3.170}$$

It is worth noting that this solution matches that of Eq. (3.142) for $\lambda = 0$.

There is also a ultra-relativistic solution where the wiggliness is able to reach scaling

$$\begin{aligned} L &= L_o t \\ v &= 1 \\ \mu &= m_o \\ \xi &= \sqrt{m_o} L_o t \end{aligned} \tag{3.171}$$

such that:

$$L_o = \frac{c\eta - c(1+\eta)m_o^{1/2}}{(4\lambda-2)m_o}, \tag{3.172}$$

$$m_o^{5/2}\left(\frac{\lambda c(1+\eta)}{4\lambda-2} + k + c(D-\eta)\right) + m_o^2\left(\frac{c\eta(3\lambda-2)}{4\lambda-2}\right) - m_o^{1/2}\left(\frac{\lambda c(1+\eta)}{4\lambda-2} + k + cD\right) + \frac{\lambda c\eta}{4\lambda-2} = 0. \tag{3.173}$$

It should be pointed out that one recovers Eq. (3.139) by considering $\lambda = 0$.

Lastly, there is also a scaling regime that implies small-scale structure growth:

$$\begin{aligned} L &= L_o t^{\alpha} \\ v &= 1 \\ \mu &= m_o t^{2-2\alpha} \\ \xi &= \sqrt{m_o} L_o t \end{aligned} \tag{3.174}$$

$$m_o^{1/2} = \frac{c(1+\eta)}{L_o(2\alpha - 4\lambda)}, \tag{3.175}$$

$$\alpha = \frac{1}{2}\frac{2c(1+\eta) + \lambda\left(4(k+cD) + c - 3c\eta\right)}{k + c(1+D)} < 1. \tag{3.176}$$

$$\gamma = \frac{2(k + c(D-\eta)) - \lambda\left(4(k+cD) + c - 3c\eta\right)}{k + c(1+D)}, \tag{3.177}$$

where if one considers Minkowski space $\lambda \longrightarrow 0$, one is able to recover the previous solution (3.143).

3.2.8 With expansion, energy losses and a running averaging scale

Considering all the dynamical mechanisms acting on the network, we find all three scaling regimes. Firstly, in the Goto-Nambu regime, we again obtain

$$\begin{aligned} L &= \frac{c}{2 - 4\lambda} t \\ v &= 1 \\ \mu &= 1 \\ \xi &= \frac{c}{2 - 4\lambda)} t. \end{aligned} \tag{3.178}$$

Secondly, we also obtain a full scaling solution

$$\begin{aligned} L &= L_o t \\ v &= 1 \\ \mu &= m_o \\ \xi &= \sqrt{m_o} L_o t, \end{aligned} \tag{3.179}$$

$$L = \frac{c(\eta - (1+\eta)m_o^{1/2})}{(3\lambda - 2\alpha)m_o - \lambda m_o^{-1}} \tag{3.180}$$

$$(\lambda - \delta)\left(\frac{1}{m_o^2} - 1\right) + \frac{1}{L_o}\left(\frac{k + c(D-\eta)}{m_o^{1/2}} - \frac{k + cD}{m_o^{5/2}} + \frac{c\eta}{m_o}\right) = 0 \tag{3.181}$$

Thirdly, we obtain a solution where the amount of wiggliness grows as the network evolves

$$\begin{aligned} L &= L_o t^{\alpha} \\ v &= 1 \\ \mu &= m_o t^{2-2\alpha} \\ \xi &= \sqrt{m_o} L_o t, \end{aligned} \tag{3.182}$$

$$L_o = \frac{c(1+\eta)}{m_o^{1/2}(2\alpha - 4\lambda)} \tag{3.183}$$

$$\alpha = \frac{1}{2}\frac{(2-\delta)c(1+\eta) + \lambda(4(k+c(D-\eta)) + c(1+\eta))}{k+c(1+D)} < 1 \tag{3.184}$$

$$\gamma = \frac{2(k+c(D-\eta)) + \delta c(1+\eta) - \lambda(4(k+c(D-\eta)) + c(1+\eta))}{k+c(1+D)}. \tag{3.185}$$

On the one hand, taking the fixed scale limit $\delta \longrightarrow 0$, we recover Eq. (3.174). On the other hand, considering Minkowski space $\lambda = 0$, yields previous solution (3.155).

Chapter 4

Conclusions and Further Work

The mathematical exploration of the landscape of scaling solutions of the wiggly model has led us to refine the physical interpretation of this model. We have managed to determine the possible scaling regimes and their underlying physical conditions, as well as to infer the role that each mechanism has on the overall evolution of the network. The landscape of possible scaling solutions is schematized in a diagram in Figure 4.1.

First of all, in Minkowski space, the network is expected to be in a trivial equilibrium solution, in the absence of energy loss mechanisms. The inclusion of a renormalization scale led to a possible regime where small-scale structure grows in time, but is compensated by a decreasing velocity, with the network's total energy density remaining constant. Furthermore, in this solution the domain of the averaging scale remains unrestricted, which is due to energy conservation. In addition, the set of solutions derived for the case of energy losses allowed us to infer the exact physical conditions that underlie each scaling regime: for values of the small-scale structure parameters such that $D > \eta$, wiggliness builds up indefinitely because the amount of generated small-scale structure is greater than the amount that is being lost; while $\eta > D$ implies constant wiggliness. It should also be emphasized that these results are in agreement with linear scaling observed in Minkowski space simulations [26, 36]. Finally, when the network is subject to both of these mechanisms, we determined that the averaging scale becomes bounded from above, as a consequence of the network losing energy. In other words, fast scale choices imply we are unable to find small-scale structure.

Second of all, in power law expanding universes, we have found that three scaling regimes for wiggliness are possible, as dictated by the expansion rate. In universes with

fast expansion rates, the Goto-Nambu solution subsists, or in other words, string networks are expected to have no wiggles. Networks are also expected to reach full scaling, where the network's energy density, velocity and wiggliness evolve towards a constant value. In the absence of other energy losses processes, this takes places in the matter era, but the presence of other mechanisms decreases the rate for which full scaling is attained. Our results also demonstrate that scaling is more easily achieved in the matter era rather than the radiation epoch, in agreement with numerical simulations [26] [31] [30]. For slow and intermediate expansion rates, small-scale structure is predicted to grow. Moreover, the behavior depicted by these three scaling regimes has also been found for chiral superconducting strings [35].

We also note that is clear that the introduction of energy loss mechanisms, either by Hubble damping or by energy transfer processes inherent to the network, forces the characteristic length scale to evolve in time, with its scaling exponent α being dictated by the small-scale structure parameters and/or the expansion rate. Conversely, in the absence of these mechanisms, energy conservation implies this length scale remains constant. This is as expected because by definition (Eq. (2.22), L is simply a measure of the total energy of the network. However, it is interesting to note that when acting individually on the network, each of these mechanisms has a different effect on the evolution of the correlation length. As depicted by the set of solutions (3.9), (3.20), when the network's wiggliness is constant, both length scales are in linear scaling. However, small-scale structure growth seems to have different implications depending on what the dominant energy loss mechanism is. It is clear from Eq. (3.12), that when the network is subject to energy losses only and wiggliness grows in time, L scales according to an α power specified by the energy loss parameters, while ξ still maintains its linear scaling. This contrasts with solution Eq. (3.22) in an expanding universe, where small-scale structure growth seems to disrupt the linear scaling of both the network's correlation length and characteristic length scale. This also further emphasizes the two-scale feature of the wiggly model, where there are two different length scales with distinct dynamics. In addition, as far as the energy loss mechanisms are concerned, it can be said that the proportionality relation between the loop chopping efficiency c and the wiggliness m_o depicted in solutions (3.13), (3.37), (3.67), (3.86) seem to suggest wiggliness increases the probability for loop production, in agreement with predictions from numerical studies [20]. Lastly, one aspect that remains unclear, and needs to be clarified in future studies, is the role of the coarse-graining scale,

and in particular, the apparent scale dependence of the total energy of the network. One would expect the way the network loses energy to not depend on the choice scale, but this is in direct contradiction with the scaling solutions we obtained.

Finally, this analytic work also aims to pave the way for a future calibration of the wiggly framework. On the one hand, the obtained scaling solutions provide a way for testing against field theory and Goto-Nambu numerical simulations. On the other hand, numerical studies will also allow for measurements of the small-scale wiggliness. Goto-Nambu simulations are of special interest for the calibration of the scaling solutions as they enable the energy loss terms associated with intercommutation and loop production to be switched off, facilitating the comparison between solutions where different physical mechanisms dominate. Despite the already existing Goto-Nambu simulations [26, 30, 31, 36, 37], a robust calibration of the wiggly model has not yet been accomplished. Having said this, our results are nevertheless qualitatively compatible with these numerical studies. Conventional CPU-based Abelian-Higgs simulations also do not provide enough spatial resolution to do this type of analysis, in spite of previous attempts [38]. The most promising route to a detailed calibration of the wiggly model is expected to come from a new generation GPU-accelerated Abelian-Higgs code [39, 40].

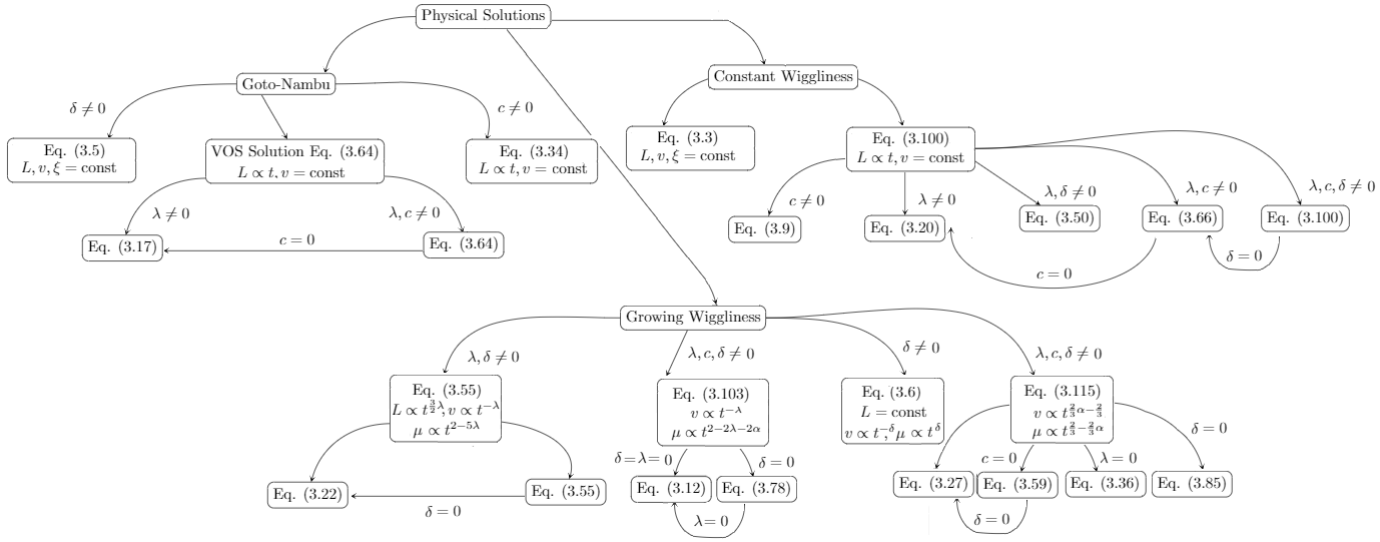

FIGURE 4.1: Schematic representation of the various families of scaling solutions.

Epilogue: Numerical Simulations

We will now proceed to a preliminary qualitative analysis of wiggliness diagnostics from numerical simulations. There are two main ways by which cosmic string networks can be simulated. Goto-Nambu simulations are based on the infinitely thin approximation that underlies the Goto-Nambu effective action, which allows for great dynamic range. The other approach is Abelian-Higgs (field theory) simulations, which consist of simulating the evolution of the underlying fields on a discrete comoving lattice, with the strings being a specific homotopic configuration of the fields. This approach, however, comes at a great computational cost, which imposes limitations on both the dynamical range and spatial resolution of the simulations.

This problem of computational limitation is evident in traditional CPU-based Abelian-Higgs simulations but lessened in GPU-based simulations. Due to the high-resolution of GPU-based codes, one is then able to characterize the small-scale structure of the network in unprecedented detail by measuring the major wiggliness diagnostics, such as the renormalized mass per unit length and the multifractal dimension. The renormalized mass per unit length can be measured by comparing the euclidean and comoving distances as a function of the scale, for pairs of points along the string. The multifractal dimension is computed by calculating $d_m(\ell) = 1 + \frac{\partial(\ln \mu)}{\partial(\ln \ell)}$.

In Figures 4.2 4.3 4.4 4.5, we show some preliminary results obtained with GPU-based simulations, in particular the measured wiggliness as a function of the conformal time η, in fixed and dynamic scales, for both matter and radiation epochs. One aspect that becomes clear is the necessity for more data, especially data that encompasses a broad range of expansion rates. Nevertheless, these results still allow us to infer some qualitative conclusions. First of all, there seems to be an overall tendency of wiggliness decrease with time for both expansion rates. For the smaller scales however, it appears that the wiggliness of the network is roughly constant. From a physical point of view, this makes sense: for large scales we expect the small-scale structure to become progressively smaller

in time, while for scales below the correlation length wiggliness should be constant. Second of all, it can be seen that, for a given time, the measured values of the wiggliness differ substantially depending on the scale at which they are being measured. This is qualitatively consistent with the fractal properties of string networks observed in Goto-Nambu simulations. More sophisticated analysis using outputs from the GPU-accelerated Abelian-Higgs simulations are expected to be made in the future, including Bayesian estimation of the small-scale structure parameters.

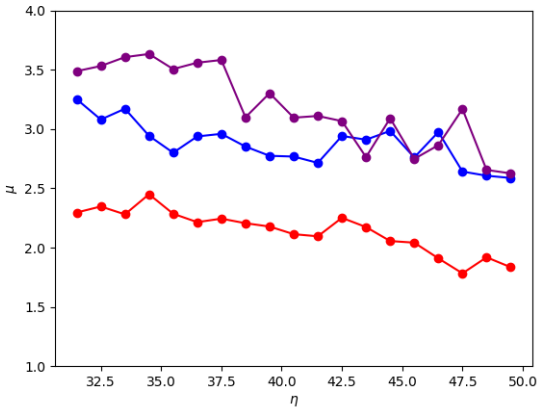

FIGURE 4.2: The wiggliness as a function of the conformal time η for a dynamic scale, for the matter era $\lambda = \frac{2}{3}$. Represented in purple, the wiggliness measured for twice the correlation length 2ξ, in blue measured at ξ level, in red measured at $\frac{\xi}{2}$.

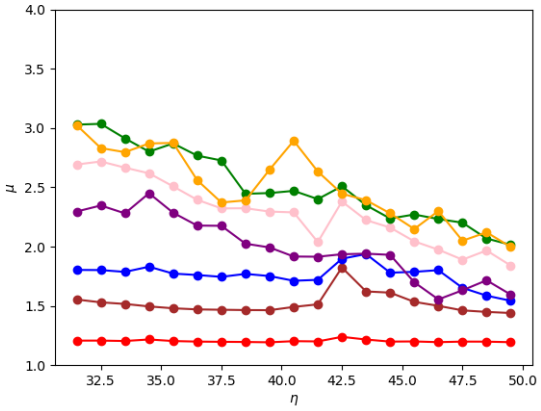

FIGURE 4.3: The wiggliness as a function of the conformal time η for a fixed scale, for the matter era $\lambda = \frac{2}{3}$. The wiggliness measured at 30 u.a (u.a. being a lattice unit) is depicted in the orange line, at 25 u.a in green, at 20 u.a in pink, at 15 u.a in purple, at 10 u.a in blue, at 5 u.a in brown, and at 1 u.a in red.

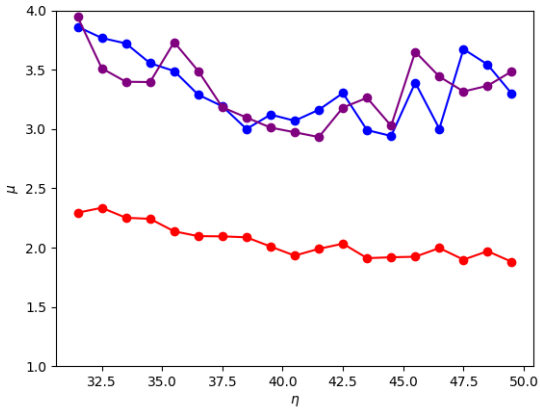

FIGURE 4.4: The wiggliness as a function of the conformal time η for a dynamic scale, for the radiation era $\lambda = \frac{1}{2}$. Represented in purple, the wiggliness measured for twice the correlation length 2ξ, in blue measured at ξ level, in red measured at $\frac{\xi}{2}$.

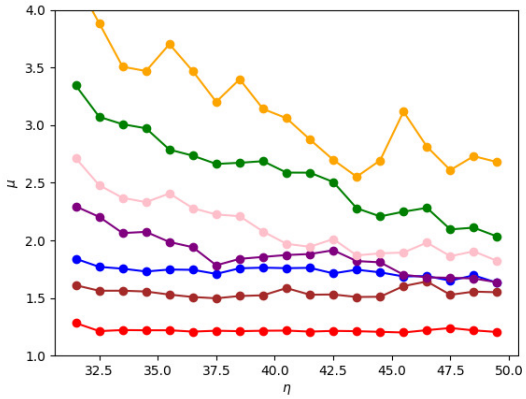

FIGURE 4.5: The wiggliness as a function of the conformal time η for a fixed scale, for the radiation era $\lambda = \frac{1}{2}$. The wiggliness measured at 30 u.a is depicted by the orange color, at 25 u.a in green, at 20 u.a in pink, at 15 u.a in purple, at $10u.a$ in blue, at 5 u.a in brown, and at 1 u.a in red.

Bibliography

[1] A. Vilenkin and E. P. S. Shellard, *Cosmic Strings and other Topological Defects*. Cambridge, U.K.: Cambridge University Press, 1994. [Cited on pages 1 and 4.]

[2] S. Weinberg, *Cosmology*. Oxford university press, 2008. [Cited on page 1.]

[3] P. A. Ade, N. Aghanim, M. Alves, C. Armitage-Caplan, M. Arnaud, M. Ashdown, F. Atrio-Barandela, J. Aumont, H. Aussel, C. Baccigalupi *et al.*, "Planck 2013 results. i. overview of products and scientific results," *Astronomy & Astrophysics*, vol. 571, p. A1, 2014. [Cited on page 4.]

[4] T. W. Kibble, "Topology of cosmic domains and strings," *Journal of Physics A: Mathematical and General*, vol. 9, no. 8, p. 1387, 1976. [Cited on pages 4 and 6.]

[5] J. Goldstone, "Field theories with «superconductor» solutions," *Il Nuovo Cimento (1955-1965)*, vol. 19, no. 1, pp. 154–164, 1961. [Cited on page 5.]

[6] C. J. Martins, *Defect evolution in cosmology and condensed matter: quantitative analysis with the velocity-dependent one-scale model*. Springer, 2016. [Cited on pages 8, 11, and 22.]

[7] R. H. Brandenberger, A.-C. Davis, and M. Hindmarsh, "Baryogenesis from collapsing topological defects," *Physics Letters B*, vol. 263, no. 2, pp. 239–244, 1991. [Cited on page 8.]

[8] S. F. Bramberger, R. H. Brandenberger, P. Jreidini, and J. Quintin, "Cosmic string loops as the seeds of super-massive black holes," *Journal of Cosmology and Astroparticle Physics*, vol. 2015, no. 06, p. 007, 2015. [Cited on page 8.]

[9] A. Vilenkin, "Cosmic strings as gravitational lenses," *The Astrophysical Journal*, vol. 282, pp. L51–L53, 1984. [Cited on page 9.]

[10] M. Sazhin, G. Longo, M. Capaccioli, J. Alcalá, R. Silvotti, G. Covone, O. Khovanskaya, M. Pavlov, M. Pannella, M. Radovich *et al.*, "Csl-1: chance projection effect or serendipitous discovery of a gravitational lens induced by a cosmic string?" *Monthly Notices of the Royal Astronomical Society*, vol. 343, no. 2, pp. 353–359, 2003. [Cited on page 9.]

[11] O. Sazhina, D. Scognamiglio, M. Sazhin, and M. Capaccioli, "Optical analysis of a cmb cosmic string candidate," *Monthly Notices of the Royal Astronomical Society*, vol. 485, no. 2, pp. 1876–1885, 2019. [Cited on page 9.]

[12] N. Kaiser and A. Stebbins, "Microwave anisotropy due to cosmic strings," *Nature*, vol. 310, no. 5976, pp. 391–393, 1984. [Cited on page 9.]

[13] J. R. Gott III, "Gravitational lensing effects of vacuum strings-exact solutions," *The Astrophysical Journal*, vol. 288, pp. 422–427, 1985. [Cited on page 9.]

[14] J. Silk and A. Vilenkin, "Cosmic strings and galaxy formation," *Physical review letters*, vol. 53, no. 17, p. 1700, 1984. [Cited on page 9.]

[15] A. Vilenkin, "Gravitational radiation from cosmic strings," *Physics Letters B*, vol. 107, no. 1-2, pp. 47–50, 1981. [Cited on page 9.]

[16] C. Hogan and M. Rees, "Gravitational interactions of cosmic strings," *Nature*, vol. 311, no. 5982, pp. 109–114, 1984. [Cited on page 9.]

[17] J. J. Blanco-Pillado, K. D. Olum, and X. Siemens, "New limits on cosmic strings from gravitational wave observation," *Physics Letters B*, vol. 778, pp. 392–396, 2018. [Cited on page 9.]

[18] B. P. Abbott, R. Abbott, T. D. Abbott, F. Acernese, K. Ackley, C. Adams, T. Adams, P. Addesso, R. X. Adhikari, V. B. Adya *et al.*, "Constraints on cosmic strings using data from the first advanced ligo observing run," *Physical Review D*, vol. 97, no. 10, p. 102002, 2018. [Cited on page 9.]

[19] C. J. A. P. Martins, E. P. S. Shellard, and J. P. P. Vieira, "Models for small-scale structure of cosmic strings: Mathematical formalism," *Phys. Rev. D*, vol. 90, p. 043518, Aug 2014. [Online]. Available: http://link.aps.org/doi/10.1103/PhysRevD.90.043518 [Cited on pages 11, 16, and 24.]

[20] J. Vieira, C. Martins, and E. Shellard, "Models for small-scale structure on cosmic strings. II. Scaling and its stability," *Phys. Rev. D*, vol. 94, no. 9, p. 096005, 2016, [Erratum: Phys.Rev.D 94, 099907 (2016)]. [Cited on pages 11, 16, 18, 21, 24, and 56.]

[21] C. Martins and E. Shellard, "Quantitative string evolution," *Physical Review D*, vol. 54, no. 4, p. 2535, 1996. [Cited on page 12.]

[22] C. J. A. P. Martins and E. P. S. Shellard, "Scale-invariant string evolution with friction," *Phys. Rev. D*, vol. 53, pp. R575–R579, Jan 1996. [Cited on page 12.]

[23] T. Kibble, "Evolution of a system of cosmic strings," *Nuclear Physics B*, vol. 252, pp. 227–244, 1985. [Cited on page 12.]

[24] D. Austin, E. J. Copeland, and T. W. B. Kibble, "Evolution of cosmic string configurations," *Physical Review D*, vol. 48, no. 12, p. 5594, 1993. [Cited on page 12.]

[25] J. Moore, E. Shellard, and C. Martins, "Evolution of abelian-higgs string networks," *Physical Review D*, vol. 65, no. 2, p. 023503, 2001. [Cited on page 12.]

[26] C. Martins and E. Shellard, "Fractal properties and small-scale structure of cosmic string networks," *Physical Review D*, vol. 73, no. 4, p. 043515, 2006. [Cited on pages 16, 17, 18, 21, 22, 28, 55, 56, and 57.]

[27] J. Correia and C. Martins, "Extending and calibrating the velocity dependent one-scale model for cosmic strings with one thousand field theory simulations," *Physical Review D*, vol. 100, no. 10, p. 103517, 2019. [Cited on page 22.]

[28] J. R. C. C. C. Correia and C. J. A. P. Martins, "Quantifying the effect of cooled initial conditions on cosmic string network evolution," *Phys. Rev. D*, vol. 102, p. 043503, Aug 2020. [Cited on page 12.]

[29] C. J. A. P. Martins and E. P. S. Shellard, "Extending the velocity-dependent one-scale string evolution model," *Phys. Rev.*, vol. D65, p. 043514, 2002. [Cited on pages 13 and 14.]

[30] B. Allen and E. Shellard, "Cosmic-string evolution: A numerical simulation," *Physical review letters*, vol. 64, no. 2, p. 119, 1990. [Cited on pages 17, 56, and 57.]

[31] D. P. Bennett and F. R. Bouchet, "High-resolution simulations of cosmic-string evolution. i. network evolution," *Physical Review D*, vol. 41, no. 8, p. 2408, 1990. [Cited on pages 17, 56, and 57.]

[32] H. Takayasu, *Fractals in the physical sciences*. Manchester University Press, 1990. [Cited on page 18.]

[33] C. Martins, J. Moore, and E. Shellard, "Unified model for vortex-string network evolution," *Physical review letters*, vol. 92, no. 25, p. 251601, 2004. [Cited on page 22.]

[34] A. Almeida and C. Martins, "Scaling solutions of wiggly cosmic strings," *Physical Review D*, vol. 104, no. 4, p. 043524, 2021. [Cited on page 22.]

[35] M. Oliveira, A. Avgoustidis, and C. Martins, "Cosmic string evolution with a conserved charge," *Physical Review D*, vol. 85, no. 8, p. 083515, 2012. [Cited on pages 28 and 56.]

[36] M. Sakellariadou and A. Vilenkin, "Cosmic-string evolution in flat spacetime," *Physical Review D*, vol. 42, no. 2, p. 349, 1990. [Cited on pages 55 and 57.]

[37] J. J. Blanco-Pillado, K. D. Olum, and B. Shlaer, "Large parallel cosmic string simulations: New results on loop production," *Physical Review D*, vol. 83, no. 8, p. 083514, 2011. [Cited on page 57.]

[38] M. Hindmarsh, S. Stuckey, and N. Bevis, "Abelian higgs cosmic strings: Small-scale structure and loops," *Physical Review D*, vol. 79, no. 12, p. 123504, 2009. [Cited on page 57.]

[39] J. Correia and C. J. Martins, "Abelian-higgs cosmic string evolution with cuda," *Astronomy and Computing*, vol. 32, p. 100388, 2020. [Cited on page 57.]

[40] J. R. C. C. C. Correia and C. J. A. P. Martins, "Abelian–higgs cosmic string evolution with multiple gpus," *Astronomy and Computing*, vol. 34, p. 100438, 2021. [Cited on page 57.]